Astron Astrophys Rev (2009) 17:251–308
DOI 10.1007/s00159-009-0020-6

REVIEW ARTICLE

Starspots

Klaus G. Strassmeier

Received: 16 December 2008 / Published online: 2 May 2009

Abstract Starspots are created by local magnetic fields on the surfaces of stars, just as sunspots. Their fields are strong enough to suppress the overturning convective motion and thus block or redirect the flow of energy from the stellar interior outwards to the surface and consequently appear as locally cool and therefore dark regions against an otherwise bright photosphere (Biermann in Astronomische Nachrichten 264:361, 1938; Z Astrophysik 25:135, 1948). As such, starspots are observable tracers of the yet unknown internal dynamo activity and allow a glimpse into the complex internal stellar magnetic field structure. Starspots also enable the precise measurement of stellar rotation which is among the key ingredients for the expected internal magnetic topology. But whether starspots are just blown-up sunspot analogs, we do not know yet. This article is an attempt to review our current knowledge of starspots. A comparison of a white-light image of the Sun (G2V, 5 Gyr) with a Doppler image of a young solar-like star (EK Draconis; G1.5V, age 100 Myr, rotation $10 \times \Omega_{\rm Sun}$) and with a mean-field dynamo simulation suggests that starspots can be of significantly different appearance and cannot be explained with a scaling of the solar model, even for a star of same mass and effective temperature. Starspots, their surface location and migration pattern, and their link with the stellar dynamo and its internal energy transport, may have far reaching impact also for our understanding of low-mass stellar evolution and formation. Emphasis is given in this review to their importance as activity tracers in particular in the light of more and more precise exoplanet detections around solar-like, and therefore likely spotted, host stars.

Keywords Starspots · Stars: activity · Stars: imaging · Sunspots · Magnetic fields · Techniques: polarimetric · Stars: rotation · Exoplanets

K. G. Strassmeier (✉)
Astrophysikalisches Institut Potsdam (AIP), An der Sternwarte 16,
14482 Potsdam, Germany
e-mail: kstrassmeier@aip.de
URL: http://www.aip.de

1 History

The basic idea that became known as the "starspot hypothesis" is the existence of large cool spots or spot groups on the surfaces of other stars (Fig. 1). This hypothesis goes back to 1667 when the French astronomer Ismael Boulliau (1605–1694) used it in his *Ad Astronomos Monita Duo* to explain the periodic light variability of Omicron Ceti (Mira). Although a wrong explanation in this case, it was the first time it appeared in the literature. Photometric observations of stars with actually existing starspots, although also not known at that time, date back to 1940s when Kron (1947) observed four eclipsing binaries and detected significant light variability outside eclipse that could not be explained. These stars were later called RS CVn binaries. Finally, Hall (1972) explicitly postulated the starspot model to explain these wave-like features in the light curves of rotating RS CVn stars due to dark starspots moving in and out of view. In parallel, European and Russian astronomers had reached the same conclusion more or less independently (Hoffmeister 1965; Chugainov 1966; Catalano and Rodonó 1967). The NASA/Harvard ADS database now lists 368 articles (from 1972 to April 2009) with the word "starspot(s)" in the title, and a total of 1,296 articles mentioned it in the abstract.

2 International conferences

Although there were numerous conferences that dealt with stellar activity in general, and in splinters also with starspot-related issues, only three recent meetings explicitly focussed on starspots: the celebration of the 200th anniversary of the Armagh Observatory in 1990 was commemorated with a scientific meeting on "*Surface inhomogeneities on late-type stars*" (Byrne and Mullan 1990, Springer-Verlag). Then,

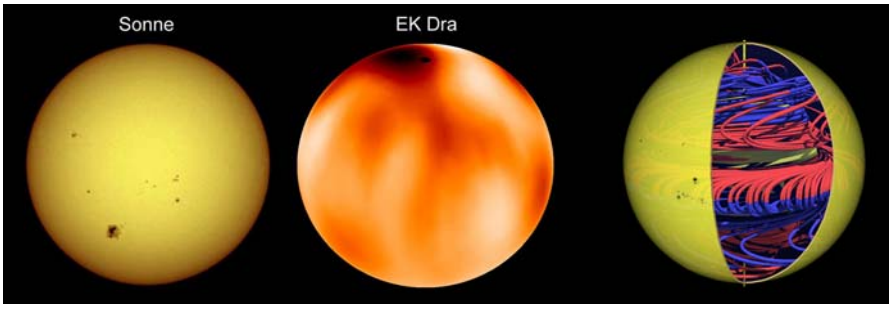

Fig. 1 The Sun (*left*) and EK Draconis (*middle*). A comparison of the Sun with a young solar analogue of age approximately 100 Myr and a rotation period ten times faster than the current Sun shows cool spots of much larger dimension and also at higher latitudes than their solar counterparts. Note that the *single black dot* in the EK Dra image indicates the position of the pole of the rotation axis, and is not a spot. Based on data from Strassmeier and Rice (1998a). *Right* a boundary-layer mean-field dynamo produces a dipole-like magnetic field structure. The simulation shows magnetic field lines with a dipole-like field structure. *Blue* means pointing inward, *red* means pointing outward. Individual flux-tube bundles may reach the stellar surface and then emerge as bipolar spot groups. The rotation axis is indicated. Simulation courtesy of Rainer Arlt, AIP

in 1995, the 176th IAU Symposium was held in Vienna under the headings of "*Stellar surface structure*" (Strassmeier and Linsky 1996, IAU Symp. 176, Kluwer Publ.) and, more recently, was the 1st Potsdam ThinkShop on "*Sunspots and starspots*" held in Potsdam in May 2002 (Strassmeier, Washuettl and Schwope 2002, AN 323, 155). A total of 49 research papers or reviews on the subject were presented in that proceedings issue of AN ("Astronomische Nachrichten", published by Wiley-VCH), which still represents a valuable collection of papers on the topic. It was also the start of the Potsdam ThinkShop series that featured another starspot-related meeting in 2007 on "*Meridional flow, differential rotation, solar and stellar activity*". This proceedings papers appeared in AN 328, issue #10[1] (edited by G. Rüdiger and R. Arlt) and I refer the reader to these issues and the original literature cited therein. The IAU just announced the acceptance of an IAU Symposium on "The physics of Sun and Starspots" to be held in Los Angeles in August 2010 (IAU Symposium #273). Besides, there are two recent review papers, one explicitly on "*Starspots*" and one on "*The sun in time*", both as part of the Max–Planck-Society's "Living reviews" series (Berdyugina 2005; Güdel 2007, respectively). An earlier review on "*Sunspots: an overview*" was given by Solanki (2003). Another recent addition was the monograph "*Sunspots and starspots*" by Thomas and Weiss (2008) at Cambridge University Press, all of which I very much recommend for a more extended consultation on various subtopics. Historically, it is interesting to compare our current standing to the earlier reviews, e.g. to that by Vogt (1981a) "*Starspots—a review of observations and theory*" from the early days of starspot research.

3 Cosmic magnetic fields: a motivation for starspot research

Magnetic processes just like those seen on the Sun have now slowly moved to centre stage in other astrophysical areas. The application to other stars opened up a new field of research that became widely known as the solar–stellar connection. Late-type stars with convective envelopes are all affected by magnetic processes which give rise to a rich variety of phenomena on their surface (e.g. Donati et al. 2006a) as well as in their environment that may affect close-in planets and even back-react on to the star (e.g. Shkolnik et al. 2003; Catala et al. 2007; Kashyap et al. 2008; Lanza 2008). Magnetic fields are likely to play a crucial role in the accretion process of T-Tauri stars as well as in the acceleration and collimation of jet-like flows in young stellar objects. Another area is the physics of accreting black holes, where magnetic activity is now believed to be responsible for most of the behaviour of these objects, including their X-ray spectrum, their notoriously dramatic variability, and the powerful relativistic jets they produce. Another area is the physics of the central engines of cosmic gamma-ray bursts, the most powerful explosions in the current universe. The main ingredient for explaining these events invokes powering and focussing of the bursts by magnetic fields. It is fair to say that virtually all the physics of magnetic fields exploited in these areas of astrophysics is based directly on our understanding of the Sun's magnetic

[1] http://www3.interscience.wiley.com/journal/117872565/issue.

field (see, e.g. Schrijver and Zwaan 2000; Stenflo 2004; Solanki 2004; Rüdiger and Hollerbach 2004; Wielebinski and Beck 2005).

4 How many spotted stars are there?

Most likely, all cool stars, either fully convective or with a convective envelope like the Sun, will have spots on their surfaces. The number of stars with spots in our galaxy should thus exceeds 200 billion, most of them not detectable with current techniques though.

So far, some 500 spotted stars have been analysed in one or the other way and the observations also published. Photometric surveys for other purposes, e.g. the search for microlensing events (OGLE; Wozniak et al. 2005) or planetary transits and therealike (e.g. ASAS; Pojmanski 2005) just to name two, have produced thousands or even tens of thousands of light curves of rotating stars with starspots but were not analysed as such. Heyrovský and Sasselov (2000) and Hendry et al. (2002) examined the photometric microlensing signatures of photospheric starspots and concluded that well-sampled multi-bandpass light curves of good photometric precision of such events could detect starspots. The presence of starspots could even mimic a low-mass companion of the lens in some events. The most likely lens sources would be low-mass stars within a few hundred pc. Along the same lines, Guinan et al. (1997) suggested that almost all of the "miscellaneous" variable stars found in the OGLE microlensing survey are actually spotted, chromospherically active stars.

Similar spin-off has been achieved from the radial-velocity-based searches for exoplanets. For example, the Keck–Lick planet search provided CaII H&K S values for 1,228 F-M stars. On this basis, Wright et al. (2004) found that most of the stars previously identified as Maunder Minimum stars from Mount Wilson Observatory S-index data are in fact older stars that had already evolved off the main sequence and intrinsically have lower H&K emission-line fluxes.

A catalogue of spotted stars does not exist but a basis is the second edition of the "Catalog of chromospherically active binary stars" (Strassmeier et al. 1993a,b) that contains 206 entries and 124 candidates. Updates of this catalog were collected over the years by Eker et al. (2008, private communication) and have now reached 372 entries.

5 Direct spot detections

Hubble space telescope (HST) imaging of the M2 supergiant Betelgeuse (α Orionis) has shown a bright spot in ultraviolet wavelengths (Fig. 2; Gilliland and Dupree 1996) and in particular in MgII H&K, i.e. located in the star's dynamic chromosphere above the photosphere. Although not dubbed a "starspot" in the sense of a sunspot analogue it was the first direct detection of stellar surface inhomogeneity on a star other than the Sun. However, it was already seen in images from optical interferometry with the 4.2-m William Herschel telescope (WHT) at 710 nm (TiO bandhead) as early as 1989 by Buscher et al. (1990) and later followed up by other ground- and space-based observations (for a summary of existing images see Freytag et al. 2002). Newer observations

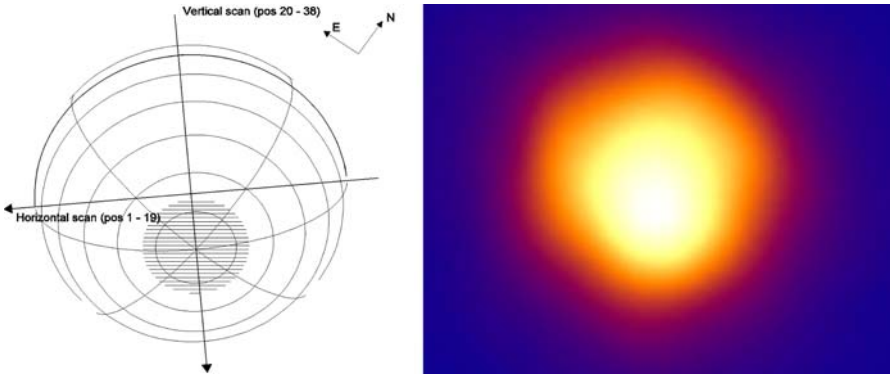

Fig. 2 A HST image of the surface of the red supergiant Betelgeuse (*right*). The star has a photospheric radius of approximately 800 solar radii and a chromospheric radius of about twice that. The latter is very dynamic with an average expansion velocity of 10 km/s. The bright feature in the *right* image somewhat off centre may be a single spot and has been explained to be either a granulation cell, a certain non-spherical pulsation mode, but also an enhanced outflow structure, e.g. as in a magnetic solar-like plage (Gilliland and Dupree 1996)

with HST/STIS combined with ground-based optical and near-IR data suggested that the inhomogeneity is more likely an enhanced chromospheric outflow structure (Lobel et al. 2004).

So far, numerous interferometric detections of non-sphericity of very late-type cool giants have been reported in the literature, among them AGB stars, Mira's, and Carbon stars but also at least one very rapidly rotating Be star. A list of resolvable giants with predicted surface activity was given in Wittkowski et al. (2002). Early images reconstructed with bispectrum speckle interferometry were obtained for VY CMa by Wittkowski et al. (1998) and, e.g. with the very large telescope interferometer (VLTI) for the Mira variable *S* Ori, also by Wittkowski et al. (2008). However, none of these interferometric images have revealed cool or even magnetic spots so far but optical stellar interferometry with closure phase techniques likely has the potential to detect surface features like cool spots on a few active and large class-III giants. A recent attempt made by Le Bouquin et al. (2008) reported first measurements on the diameter(s) of the single M4III star V3879 Sgr with the interferometric AMBER instrument linked with ESO's VLTI fringe-tracking facility FINITO.

6 Stellar rotation and starspots

An important aspect in the evolutionary scenario of cool stars is their rotation. Theoretical models already developed make definite and testable predictions of how rotation changes with mass and age (e.g. Barnes et al. 2001). Rotational measurements throughout the entire H–R diagram are very much needed either to confirm or falsify these models. Stars with spots provide a simple mechanism to do so. Dark spots are being carried across the stellar disk by the stellar rotation and thus modulate the total brightness with the rotational period of the star. This allows to determine stellar

rotation periods with high precision and, moreover, represent superior measurements of rotation rates with respect to spectroscopic ($v \sin i$) measurements because they are independent of the (unknown) inclination of the rotational axis.

Unfortunately, deriving rotation periods is labour-intensive because constructing a light curve involves observations spread out over several weeks for sufficient temporal coverage, for the longer periods even for months. Consequently, the available dataset in the literature is biased towards faster rotators with short periods. Also, because young stars are more active than old ones, a larger fraction of the young ones have detectable photometric variations, and thus the period measurements are heavily skewed towards younger stars instead of being widely dispersed in age. An impressive study of M35 (140 Myr) from a 5-month-long time-series survey was recently presented by Meibom et al. (2008). A deep look into M37 (550 Myr) was published recently (Hartman et al. 2008). However, only one study (Radick et al. 1987) has been successful in deriving periods for a reasonable sample of stars in a much older cluster, namely the Hyades (625 Myr). Recent photometry of Praesepe (700 Myr) by Scholz and Eislöffel (2007) aimed at its very low-mass stars and brown dwarfs and would, if continued, present a very interesting extension for the more common solar-like stars.

7 Stellar differential rotation from starspot tracings

Measurements of the rotational period of stars with spots also allow the detection of differential surface rotation (Hall 1972; Baliunas et al. 1985; Strassmeier and Bopp 1992; Messina et al. 1999; Oláh et al. 2003; Walker et al. 2007). If the latitudinal location of a spot were known and, if there were spots at different latitudes, then surface rotation could be measured directly as a function of stellar latitude. The default though is that the latitude is not known. Then, the difference of the longest and shortest period observed must be taken as an estimate of the averaged amount of surface differential rotation (Hall and Busby 1990). Unfortunately, such measurements are affected by complex spot distributions, active region growth and decay, local migration due to, e.g. diffusion, spot cycles, etc., that all can either mask out the differential-rotation signal or even introduce a spurious signal. Moreover, any one-dimensional analysis, i.e. an analysis based on disk-integrated data like time-series photometry, cannot resolve the ambiguity of whether the polar or the equatorial regions rotate faster or slower. One way out is to spatially resolve the stellar disk and then trace individual spots, just as Galileo, Scheiner, and others had done for the Sun 400 years ago. This allows, in principle, not only to detect the sign of differential rotation but also to follow the spot evolution directly. The technique to do so is called Doppler imaging.

The basis for its application is that cool spots on the stellar surface give rise to clearly discernible distortions of absorption line profiles. These distortions move from blue to red wavelengths across the line profile as the spots rotate across the visible hemisphere due to stellar rotation. The span of migration within the line profile reveals the feature's latitude; it is better determined the shorter the integration time and the more numerous the spectra per rotation cycle. However, spots may evolve within a few stellar rotations, maybe even from one rotation cycle to the next, as on the Sun, or even shorter. Therefore, "missing" phases from another rotational cycle cannot just

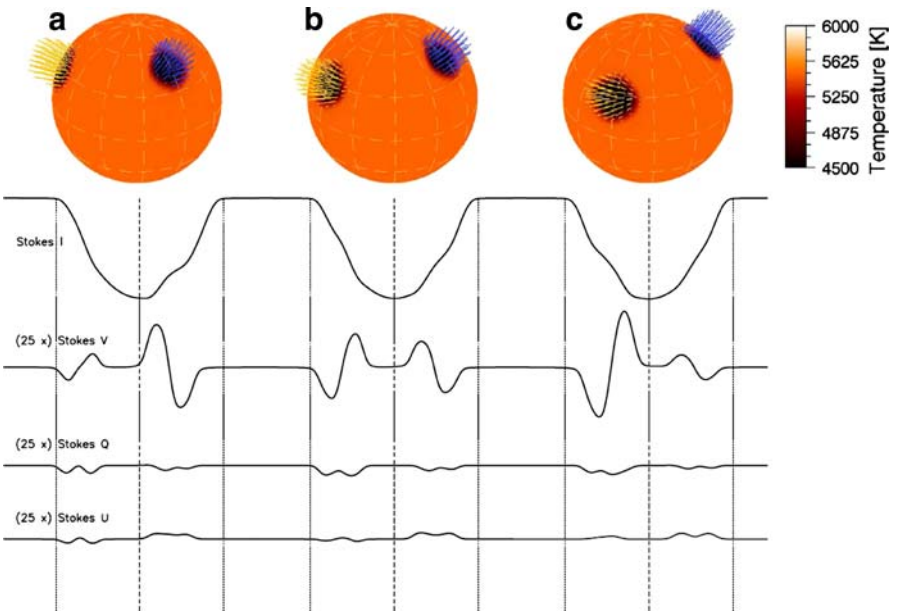

Fig. 3 The principle of (Zeeman)–Doppler imaging of cool starspots. The basis is a rotating star whose cool spots cause reduced line absorption at the wavelengths that are proportional to the Doppler velocity at their respective surface location. This reduced absorption appears as an "emission bump" in the absorption line profile. Because the rotational Doppler shift is related with the surface position of the spot with respect to the rotational axis, the technique allows the reconstruction of the spot's location and size. If the bumps migrate with different rates through the line profile and, if the latitude of the spots is constrained by the data, then it allows the determination of a surface differential rotation law. When applied to time series of polarized spectral line profiles, as shown in the figure, even the full geometry of the magnetic field can be reconstructed uniquely. For clarity in the figure, we show just three rotational phases of a hypothetical star with two spots cooler by 1,270 K relative to the surrounding photosphere and at two different latitudes. Both spots harbour a radial magnetic field of 1.5 kG, but in opposite direction. The star is shown at three rotational phases different by 18° (0.05 phases of the rotational period) and with an inclination of the rotational axis of 60°. The respective (forward) Stokes I, V, Q and U profiles (enlarged by a factor 25 with respect to Stokes I) are depicted in the *lower panels* that indicate the respective sensitivity to field inclination and strength and their modulation due to stellar rotation. See text. **a** Phase 0°, **b** Phase 18°, **c** Phase 36°

be added into the data vector as, e.g. is the case for the stable chemically peculiar Ap stars. All this makes Doppler imaging of cool stars a difficult and time-consuming technique. Figure 3 illustrates the principle with a synthetic star with two spots each harbouring a kG field of opposite direction. For further technical details, see, e.g. the reviews by Rice (2002) or Piskunov and Rice (1993).

8 Starspot detections from Doppler imaging

Table 1 is a list of cool stars that have—so far—been investigated with the Doppler-imaging technique and that have had their spots detected and mapped. Table 2 is a listing of all individual published and soon-to-be published (photospheric) Doppler images of spotted, late-type stars. This table is continuously updated at our group's

Table 1 Late-type stars with Doppler images (as of 2008)

MK-class	Star name	Type	$T_{\rm eff}$ (K)	$P_{\rm rot}$ (days)	$v_{\rm equ}$ (km/s)	R ($R_\odot$)
K2III	HD31993	Single	4,500	25.3	36.6	18.3
G9II-III	HD218153	RS CVn	4,700	24.96	31.1	15.3
K2III	IM Peg	RS CVn	4,450	24.65	30.6	14.9
K0III	HK Lac	RS CVn	4,800	24.46	22.1	10.7
K0III	XX Tri	RS CVn	4,750	24.00	24.2	11.5
G8III	HD208472	RS CVn	4,900	22.40	29.7	13.1
K1III	σ Gem	RS CVn	4,500	19.60	31.8	12.3
K1III	ζ And	RS CVn	4,600	17.77	45.7	16.0
G8III-II	CM Cam	Eff.-s	4,950	16.00	54.3	17.2
K0III-IV	IL Hya	RS CVn	4,700	12.70	32.4	8.1
K0III-IV	HU Vir	RS CVn	5,000	10.40	27.6	5.7
K2III	YY Men	FK Com	4,950	9.55	65.3	12.3
M0	DF Tau	CTTS	3,750	8.50	28.9	4.8
K2-3IV	IN Vir	RS CVn	4,600	8.23	27.7	4.5
K7	BP Tau	CTTS	4,055	7.6	12.7	2.0
K0III-IV	DM UMa	RS CVn	4,500	7.50	40.4	6.0
K2IV	II Peg	RS CVn	4,600	6.72	25.4	3.4
K5	V2129 Oph	CTTS	4,500	6.53	20.5	2.6
K0IV	UX Ari	RS CVn	4,750	6.44	45.0	5.7
G5III	IN Com	CBPN	5,200	5.91	94.8	11.1
K0III	Par 1724	WTTS	5,000	5.68	80.4	9.0
K0III	UZ Lib	RS CVn	4,800	4.77	87.5	8.2
K2IV	Sz 68	CTTS	4,800	3.90	42.6	3.3
K0-2IV	V1355 Ori	RS CVn	4,750	3.86	53.5	4.1
G5III-IV	HD199178	FK Com	5,450	3.32	93.3	6.1
F7V	τ Boo	Single	6,360	3.31	24.7	1.5
G5IV	TY Pyx A	BY Dra	5,400	3.20	35.0	2.2
G5IV	TY Pyx B	BY Dra	5,400	3.20	35.0	2.2
G2III	SU Aur	CTTS	5,800	2.90	73.9	4.2
K1IV	V711 Tau	RS CVn	4,800	2.84	75.3	4.2
K4IV	CF Tuc	RS CVn	4,500	2.80	38.9	2.2
M0-1	V830 Tau	WTTS	4,000	2.75	34.5	1.9
G2	SU Aur	CTTS	5,700	2.7	68.	3.6
G1.5V	EK Dra	Single	5,870	2.60	20.0	1.0
K0V	AG Dor	BY Dra	4,900	2.56	22.0	1.1
G4III	FK Com	FK Com	5,080	2.40	179.0	8.5
G5IV	EI Eri	RS CVn	5,500	1.945	70.9	2.7
K4IV	V410 Tau	WTTS	4,400	1.872	85.0	3.1
K2V	PW And	Single	5,000	1.761	33.2	1.2
G5IV	V824 Ara A	WTTS	5,400	1.680	48.3	1.6

Table 1 continued

MK-class	Star name	Type	$T_{\rm eff}$ (K)	$P_{\rm rot}$ (days)	$v_{\rm equ}$ (km/s)	R ($R_\odot$)
K0V-IV	V824 Ara B	WTTS	5,050	1.680	44.4	1.5
K2V	LQ Hya	Single	5,200	1.601	30.9	1.0
G5IV	HD283572	WTTS	5,250	1.549	136.0	4.2
G1-2V	HII 314	Pleiad	5,845	1.470	50.5	1.5
G0V	HD171488	Single	5,800	1.337	41.9	1.1
F9V	σ^2 CrB A	BY Dra	6,000	1.157	55.4	1.1
G0V	σ^2 CrB B	BY Dra	5,900	1.157	55.4	1.1
K0V-IV	PZ Tel	WTTS	5,000	0.9400	75.0	1.4
dM1e	YY Gem A	BY Dra	4,000	0.8143	48.1	0.8
dM1e	YY Gem B	BY Dra	4,000	0.8143	48.1	0.8
G8III-IV	LW Hya	CBPN	4,900	0.7630	127.3	1.9
G5-6V	AP 193	Alp Per	5,500	0.7480	78.1	1.2
G0V	ER Vul A	BY Dra	5,900	0.6980	92.3	1.3
G5V	ER Vul B	BY Dra	5,750	0.6980	92.3	1.3
G5-8IV/V	BV Cen	CV	5,250	0.6112	119.3	1.4
G6V	He 520	Alp Per	5,620	0.6038	98.2	1.2
G2V-IV	SV Cam	RS CVn	5,750	0.5900	117.0	1.4
G2V	HD307938	Single	5,800	0.5641	106.0	1.2
K7	TWA 6	WTTS	4,000	0.5409	98.4	1.0
K2V	V471 Tau	Pre-CV	5,000	0.5211	91.0	0.9
K0V	AB Dor	Single	5,250	0.5148	105.1	1.1
G2-3V	He 699	Alp Per	5,750	0.4908	118.7	1.2
M1-2V	EY Dra	Single	3,900	0.4586	66.0	0.6
M4V	V374 Peg	Single	3,200	0.4456	38.8	0.34
M0	MN Lup	CTTS	3,800	0.439	103.7	0.9
M1.5V	HK Aqr	Single	3,870	0.4307	69.0	0.6
K5-7V	LO Peg	Single	4,300	0.4236	120.3	1.0
K0V	HII 3163	Pleiad	5,250	0.4180	82.5	0.7
K3-5IV/V	AE Aqr	CV	4,800	0.4116	?	?
K4V	HII 686	Pleiad	4,500	0.3970	82.4	0.6
K3V	HD197890	WTTS	5,000	0.3800	156.3	1.2
G0V	AE Phe A	W UMa	6,000	0.3624	145.2	1.0
F8V	AE Phe B	W UMa	6,150	0.3624	95.1	0.7
G8V	AP 149	Alp Per	5,500	0.3200	204.0	1.3
G9V	YY Eri A	W UMa	5,400	0.3125	161.6	1.0
G7V	YY Eri B	W UMa	5,580	0.3125	111.1	0.7
G2V-IV	RXJ1508.6	Single	5,750	0.3100	245.0	1.5
?	V426 Oph	CV	?	0.2854	?	?
G9V	VXR45A	Single	(5,300)	(0.18)	238	(0.8)

Table 2 Doppler images of late-type stars (as of 2008)

Star Epoch	Type[a] ΔV	$P_{\rm rot}$ i	$v \sin i$ Spots[b]	M–K class References
HD 31993	Single	25.3	33.2	K2 III
Nov 1996	0.01	65°	H, L	Strassmeier et al. (2003a)
Nov 1996	0.01	65°	H, L	Strassmeier et al. (2003a)
KU Peg	RS CVn	24.96	28.2	G9 II-III
Nov 1996	0.07 mag	50°	P, H	Weber and Strassmeier (2001)
Dec 1996	0.04	50°	P, H	Weber and Strassmeier (2001)
IM Peg	RS CVn	24.65	26.5	K2 III
Aug 1996	?	70°	H	Berdyugina et al. (2001a)
Nov 1996	0.35	70°	H	Weber (2004)
Dec 1996	?	70°	H	Berdyugina et al. (2001a)
Dec 1996	0.35	70°	H	Weber (2007)
Aug 1997	0.2	70°	H	Berdyugina et al. (2001a)
Dec 1997	…	70°	H	Berdyugina et al. (2001a)
Jul 1998	…	70°	H	Berdyugina et al. (2001a)
Sep 1998	…	70°	H	Berdyugina et al. (2000a,b)
Jul 1999	…	70°	H	Berdyugina et al. (2000a,b)
Sep 1999	…	70°	H	Berdyugina et al. (2000a,b)
Aug 2003	…	70°	P, H, L	Marsden et al. (2007)
May 2005	…	70°	P, H, L	Marsden et al. (2007)
31images	…	70°		Marsden et al. (2007)
HK Lac	RS CVn	24.4	20	K0III
Nov 1996	0.1	65°	H, L	Weber et al. (2001)
Dec 1996	0.08	65°	H, L	Weber et al. (2001)
Jan 1997	0.05	65°	H, L	Weber et al. (2001)
Jan 1998	0.27	65°	H, L	Weber et al. (2001)
XX Tri	RS CVn	24.0	21	K0 III
Dec 1997	0.63	60°	P-H, Lw	Strassmeier (1999)
HD208472	RS CVn	22.4	21	G8III
Nov 1996	0.12	35°	H, L	Weber (2004)
N/D 1996	0.12	35°	H, L	Weber (2004)
Dec 1996	0.12	35°	H, L	Weber (2004)
σ Gem	RS CVn	19.6	27.5	K1 III
Dec 1991	0.17	60°	H, L	Hatzes (1993)
Nov 1996	0.10	60°	H, L	Kővári et al. (2001)
No/De 96	0.09	60°	H, L	Kővári et al. (2001)
Dec 1996	0.09	60°	H, L	Kővári et al. (2001)
De/Ja 96/97	0.08	60°	H, L	Kővári et al. (2001)
ζ And	RS CVn	17.7695	41.4	K1 III
Nov 1996	0.10	65°	P, L	Kővári et al. (2007a,b)

Table 2 continued

Star Epoch	Type[a] ΔV	P_{rot} i	$v \sin i$ Spots[b]	M–K class References
Nov 1996	0.10	65°	P, L	Kővári et al. (2007a,b)
Dec 1996	0.10	65°	P, L	Kővári et al. (2007a,b)
Dec 1996	0.10	65°	P, L	Kővári et al. (2007a,b)
Jan 1998	0.05	65°	P, L	Kővári et al. (2007a,b)
CM Cam	Eff.-single	16.0	47	G8 III-II
Mar 1994	0.05	60°	P, H, L	Strassmeier et al. (1998)
Mar 1995	…	60°	P, H, L	Strassmeier et al. (1998)
Jan 1996	0.05	60°	H, L	Strassmeier et al. (1998)
Apr 1997	0.02	60°	H, L	Strassmeier et al. (1998)
IL Hya	RS CVn	12.9	26.5	K0 III-IV
Mar 1994	0.10	55°	P, H, L	Weber and Strassmeier (1998)
Mar 1995	0.17	55°	P, H, L	Weber and Strassmeier (1998)
Nov 1996	0.20	55°	H, L	Weber (2004)
N/D 1996	0.20	55°	H, L	Weber (2004)
Dec 1996	0.20	55°	H, L	Weber (2004)
D/J 97/98	0.15	55°	P, H, L	Weber (2004)
Mar 2000	0.08	55°	P, H, L	Weber (2004)
Apr 2000	0.12	55°	P, H, L	Weber (2004)
HU Vir	RS CVn	10.4	25	K0 III-IV
Apr 1991	0.23	65°	P, H	Strassmeier (1994)
Apr 1991	0.23	65°	P, H	Strassmeier (1994)
Feb 1995	…	55°	P, H	Hatzes (1998)
YY Men	FK Com	9.55	50	K2 III
Jan 1987	0.3	65°	H, L	Piskunov et al. (1990)
Sep 1990	…	35°	P, L	Kürster and Dennerl (1993)
DF Tau	CTTS	8.5	25	M0
Nov 1994	…	60°	HLw	Unruh et al. (1998)
IN Vir	RS CVn	8.23	24	K2-3 IV
Mar 1994	0.16	60°	P, L	Strassmeier (1997)
BP Tau	CTTS	7.6	9	K7 IV
Feb 2006	…	45°	H	Donati et al. (2008b)
Dec 2006	…	45°	H	Donati et al. (2008b)
DM UMa	RS CVn	7.50	26	K0-1 IV-III
Jan 1993	0.2	40°	P, L	Hatzes (1995a)
II Peg	RS CVn	6.724	23	K2 IV
Aug 1992	?	60°	H	Berdyugina et al. (1998)
Oct 1992	…	65°	P, H, L	Hatzes (1995b)
Sep 1993	…	65°	P, H, L	Hatzes (1995b)
Oct 1993	0.27	60°	H	Zboril et al. (1998)

Table 2 continued

Star Epoch	Type[a] ΔV	$P_{\rm rot}$ i	$v \sin i$ Spots[b]	M–K class References
Dec 1993	…	60°	H	Berdyugina et al. (1998)
Jul 1994	?	60°	H	Berdyugina et al. (1998)
Sep 1994	…	65°	H, L	Hatzes (1995b)
Nov 1994	…	60°	H	Berdyugina et al. (1998)
Jan 1995	…	60°	H	Berdyugina et al. (1998)
Jul 1995	?	60°	H	Berdyugina et al. (1998)
Oct 1995	…	60°	H, L	Berdyugina et al. (1998)
Jul 1996	0.27	60°	H	Berdyugina et al. (1998)
Oct 1996	0.27	60°	H	Berdyugina et al. (1998)
Nov 1996	0.30	60°	H, L	Weber (2004)
Nov 1996	0.30	60°	H, L	Weber (2004)
Dec 1996	0.30	60°	H, L	Weber (2004)
Dec 1996	0.29	60°	H, L	Weber (2004)
Jan 1997	0.28	60°	H, L	Weber (2004)
Jun 1997	0.28	60°	H, L	Berdyugina et al. (1999)
Aug 1997	0.30	60°	H	Berdyugina et al. (1999)
Dec 1997	0.35	60°	H	Berdyugina et al. (1999)
Jul 1998	0.22	60°	H, L	Berdyugina et al. (1999)
Oct 1998	0.30	60°	H	Berdyugina et al. (1999)
Nov 1998	0.30	60°	H	Berdyugina et al. (1999)
Aug 2004	…	60°	H, L	Carroll et al. (2007)
V2129 Oph	CTTS	6.53	14.5	K5 IV
Jun 2005	…	45°	P, H, L	Donati et al. (2007)
UX Ari	RS CVn	6.44	39	K0 IV
1983-1984	0.3	60°	H, L	Noah et al. (1987)
Aug 1986	…	60°	P, L	Vogt and Hatzes (1991)
Nov 1986	…	60°	P, L	Vogt and Hatzes (1991)
Jan 1987	…	60°	P, H, L	Vogt and Hatzes (1991)
Nov 1995	…	60°	H, L	Aarum et al. (1999)
Dec 1996	…	60°	H, L	Aarum et al. (1999)
IN Com	CBPN	5.91	67	G5 III
Mar 1994	0.1	45°	P, L	Strassmeier et al. (1997)
Par 1724	WTTS	5.68	71	K0 III
Jan 1996	0.35	62°	H, L	Neuhäuser et al. (1998)
Jan 1996	0.35	62°	H, L	Stout-Batalha (1997)
UZ Lib	RS CVn	4.768	67	K0 III
Mar 1994	0.10	30°	P, L	Strassmeier (1996)
Jan 1996	0.14	50°	P, L	Oláh et al. (2002)
May 1996	0.12	50°	P, L	Oláh et al. (2002)

Table 2 continued

Star Epoch	Type[a] ΔV	P_{rot} i	$v \sin i$ Spots[b]	M–K class References
Apr 1997	0.15	50°	P, L	Oláh et al. (2002)
Apr 1998	0.13	50°	P, L	Oláh et al. (2002)
Apr 1998	0.13	50°	P, L	Oláh et al. (2002)
Apr 2000	0.14	50°	P, L	Oláh et al. (2002)
May 2000	0.14	50°	P, L	Oláh et al. (2002)
Sz 68	CTTS	3.9	40	K2 IV
Jul 1995	…	70°	P, H, L	Johns-Krull and Hatzes (1997)
V1355 Ori	RS CVn	3.858	41	K0-2 IV
Apr 1997	0.18	50°	P, H	Strassmeier (2000)
Apr 1998	0.25	50°	P, H, L	Strassmeier (2000)
Feb 1999	0.06	50°	P, H, L	Strassmeier (2000)
HD199178	FK Com	3.32	70.0	G5 III-IV
1985	…	80°	P, L	Vogt (1988)
Aug 1988	0.05	40°	P, H, L	Strassmeier et al. (1999a,b)
Apr 1989	0.08	40°	P, H, L	Strassmeier et al. (1999a,b)
May 1989	0.05	40°	P, H, L	Strassmeier et al. (1999a,b)
May 1990	0.06	40°	P, H, L	Strassmeier et al. (1999a,b)
Jul 1994	0.08	60°	P-H, L	Hackman et al. (2001)
Aug 1994	0.07	60°	P-H	Hackman et al. (2001)
Nov 1994	…	60°	H	Hackman et al. (2001)
Jul 1995	0.11	60°	H, L	Hackman et al. (2001)
Apr 1997	0.12	40°	P, H, L	Strassmeier et al. (1999a,b)
Jan 1999	…	50°	P, H	Petit et al. (2004a,b)
Jul 2001	…	50°	P, H	Petit et al. (2004a,b)
Dec 2001	…	50°	P, H	Petit et al. (2004a,b)
Jun 2002	…	50°	P, H	Petit et al. (2004a,b)
J/J 2002	…	50°	P, H	Petit et al. (2004a,b)
Jul 2002	…	50°	P, H	Petit et al. (2004a,b)
J/J 2003	…	50°	P, H	Petit et al. (2004a,b)
Jul 2003	…	50°	P, H	Petit et al. (2004a,b)
J/A 2003	…	50°	P, H	Petit et al. (2004a,b)
τ Boo	Single	3.31	15.9	F7V
Jun 2006	…	40°	P, H, L	Catala et al. (2007)
Jul 2007	…	40°	H, L	Donati et al. (2008a)
TY Pyx A	BY Dra	3.20	35	G5IV
Apr 1997	…	88°	L	Piskunov et al. (2001)
TY Pyx B	BY Dra	3.20	35	G5IV
Apr 1997	…	88°	H	Piskunov et al. (2001)
SU Aur	CTTS	2.9	60	G2 III

Table 2 continued

Star Epoch	Type[a] ΔV	$P_{\rm rot}$ i	$v \sin i$ Spots[b]	M–K class References
Nov 1994	…	80°	L	Petrov et al. (1995)
Nov 1996	…	60°	H, L	Unruh et al. (2004)
V711 Tau	RS CVn	2.84	41	K1 IV
Aug 1981	0.10	33°	P, H, L	Vogt et al. (1999)
Oct 1981	0.2	33°	P, L	Vogt and Penrod (1983)
Sep 1982	0.07	33°	P, H	Vogt et al. (1999)
Sep 1983	…	33°	H	Gondoin (1986)
Oct 1984	0.07	33°	P, H, L	Vogt et al. (1999)
Oct 1985	0.08	33°	P, H	Vogt et al. (1999)
Aug 1986	0.10	33°	P, H, L	Vogt et al. (1999)
Jan 1987	0.06	33°	P, H, L	Vogt et al. (1999)
Sep 1987	0.03	33°	P, H, L	Vogt et al. (1999)
Oct 1988	0.08	33°	P, H, L,Lw	Vogt et al. (1999)
1988-91	0.1	33°	P, L	Donati et al. (1992)
Feb 1989	0.07	33°	P, H, L,Lw	Vogt et al. (1999)
Sep 1989	0.11	33°	P, H, L	Vogt et al. (1999)
Oct 1989	0.07	33°	P, H, L	Vogt et al. (1999)
Nov 1989	0.08	33°	P, H, L	Vogt et al. (1999)
Dec 1989	0.1	33°	P, L	Jankov and Donati (1995)
Sep 1990	…	33°	P, H, L	Vogt et al. (1999)
Oct 1990	…	33°	P, H, L	Vogt et al. (1999)
Dec 1990	…	33°	P, H, L	Vogt et al. (1999)
Jan 1991	0.08	33°	P, H	Vogt et al. (1999)
Oct 1991	…	33°	P, H, L	Vogt et al. (1999)
Nov 1991	…	33°	P, H, L	Vogt et al. (1999)
Dec 1991	…	44°	P, H, L	Donati (1999)
Jan 1992	…	33°	P, H, L	Vogt et al. (1999)
Sep 1992	…	33°	P, H, L	Vogt et al. (1999)
Oct 1992	0.07	33°	P, H, L	Vogt et al. (1999)
Dec 1992	0.07	33°	P, H, L	Vogt et al. (1999)
Dec 1992	…	44°	P, H, L	Donati (1999)
Dec 1992	0.06	33°	P, L	Jankov and Donati (1995)
Feb 1993	…	33°	P, H, L	Vogt et al. (1999)
Dec 1993	…	44°	P, H, L	Donati (1999)
Dec 1995	…	44°	P, H, L	Donati (1999)
Nov 1996	0.2	40°	P, H, L	Strassmeier and Bartus (2000)
No/De 96	0.2	40°	P, H, L	Strassmeier and Bartus (2000)
Dec 1996	0.2	40°	P, H	Strassmeier and Bartus (2000)
Dec 1996	…	44°	P, H, L	Donati (1999)

Table 2 continued

Star Epoch	Type[a] ΔV	P_{rot} i	$v \sin i$ Spots[b]	M–K class References
Jan 1998	…	38°	P, H, L	Donati et al. (2003)
Feb 1998	…	38°	P, H, L	Petit et al. (2004a,b)
Dec 1998	…	38°	P, H, L	Petit et al. (2004a,b)
Jan 1999	…	38°	P, H, L	Donati et al. (2003)
Jan 1999	…	38°	P, H, L	Petit et al. (2004a,b)
Dec 1999	…	38°	P, H, L	Donati et al. (2003)
Feb 2000	…	38°	P, H, L	Petit et al. (2004a,b)
Dec 2000	…	38°	P, H, L	Donati et al. (2003)
Dec 2001	…	38°	P, H, L	Petit et al. (2004a,b)
Dec 2001	…	38°	P, H, L	Donati et al. (2003)
CF Tuc	RS CVn	2.80	35	K4 IV
Oct 1990	…	64°	H, L	Kürster and Dennerl (1993)
V830 Tau	WTTS	2.75	34	M0-1
Jan 1997	0.40	80°	H, L	Hatzes (2001)
SU Aur	CTTS	2.7	59	G2
Nov 1996	yes	60°	P, L	Unruh et al. (2004)
EK Dra	Single	2.60	17.3	G1.5V
Mar 1995	0.10	60°	P, H, L	Strassmeier and Rice (1998a)
AG Dor	BY Dra	2.562	18	K0V
Nov 1992	…	55°	P, L	Washuettl and Strassmeier (2001)
FK Com	FK Com	2.400	155	G4 III
1989	…	75°	H, L	Piskunov et al. (1994)
Aug 1994	0.15	60°	H, L	Korhonen et al. (1999)
Jul 1995	0.20	60°	P-H, L	Korhonen et al. (1999)
Jul 1996	0.20	60°	H, L	Korhonen et al. (2000)
Aug 1996	0.20	60°	H, L	Korhonen et al. (2000)
Apr 1997	0.10	60°	P-H, L	Korhonen et al. (2000)
Jun 1997	0.07	60°	P-H, L	Korhonen et al. (2000)
Jan 1998	0.08	60°	P-H, L	Korhonen et al. (2001)
Apr 2008	0.15	60°	P-H, L	Korhonen et al. (2009)
EI Eri	RS CVn	1.945	51	G5 IV
Oct 1984	0.1	46°	P, H	Hatzes and Vogt (1992)
Nov 1985	0.1	46°	P, H	Hatzes and Vogt (1992)
Oct 1986	…	46°	P, H	Hatzes and Vogt (1992)
Jan 1987	…	46°	P, H	Hatzes and Vogt (1992)
Sep 1987	…	46°	P, L	Hatzes and Vogt (1992)
Dec 1987	0.05	46°	P, H	Strassmeier (1990)
Jan 1988	0.15	46°	P, H, L	Strassmeier et al. (1991)
Nov 1988	0.15	46°	P, H, L	Strassmeier et al. (1991)

Table 2 continued

Star Epoch	Type[a] ΔV	$P_{\rm rot}$ i	$v \sin i$ Spots[b]	M–K class References
Dec 1988	0.10	46°	P, H, L	Strassmeier et al. (1991)
Jan 1989	…	53°	P, H, L	Washuettl et al. (2009)
No/De 1989	…	53°	P, H, L	Washuettl et al. (2009)
Jan 1990	…	53°	P, H, L	Washuettl et al. (2009)
Oc/No 1990	…	53°	P, H	Washuettl et al. (2009)
Feb 1995	0.07	46°	P, H, L	Washuettl et al. (2009)
Jan 1996	0.09	46°	P, H, L	Washuettl et al. (2009)
Nov 1996	0.09	46°	P, H, L	Washuettl et al. (2009)
No/De 96	0.06	46°	P, H, L	Washuettl et al. (2009)
Dec 1996	0.06	46°	P, H, L	Washuettl et al. (2009)
Dec 1997	0.08	46°	P, H, L	Washuettl et al. (2009)
Nov 1998	…	46°	P, H, L	Washuettl et al. (2003) Kővári et al. (2008)
V410 Tau	WTTS	1.872	77	K4
Jan 1990	0.4	70°	P	Joncour et al. (1994b)
Nov 1992	0.37	70°	H, L	Strassmeier et al. (1994a, 1999b)
Dec 1993	0.5	70°	(P),H, L	Rice and Strassmeier (1996)
Jan 1994	…	54°	(P),H, L	Hatzes (1995d)
PW And	Single	1.7616	23.9	K2 V
Aug 2004	0.10	46°	L	Strassmeier and Rice (2006)
V824 Ara A	WTTS	1.68	37	G5 IV
Sep 1990	…	55°	P, L	Hatzes and Kürster (1999)
May 1996	0.1	50°	P, L	Strassmeier and Rice (2000)
Sep 2004	…	52°	P, H, L	Dunstone et al. (2008)
Apr 2007	…	52°	P, H, L	Dunstone et al. (2008)
V824 Ara B	WTTS	1.68	34	K0 V-IV
Sep 1990	…	55°	P, L	Kürster et al. (1992)
Sep 1990	…	55°	P, L	Hatzes and Kürster (1999)
May 1996	0.1	50°	H, L	Strassmeier and Rice (2000)
Sep 2004	…	52°	P, H, L	Dunstone et al. (2008)
Apr 2007	…	52°	P, H, L	Dunstone et al. (2008)
LQ Hya	Single	1.6007	26	K2 V
Jan 1991	0.1	70°	P-H, L	Strassmeier et al. (1993a, 1999b)
Feb 1991	…	75°	P-H, L	Saar et al. (1994)
May 1991	…	75°	H, L	Saar et al. (1994)
Dec 1991	…	55°	L	Donati (1999)
Dec 1992	…	55°	P, H, L	Donati (1999)
Dec 1993	…	55°	P, H, L	Donati (1999)
May 1993	…	75°	P, L	Saar et al. (1994)

Table 2 continued

Star Epoch	Type[a] ΔV	P_{rot} i	$v \sin i$ Spots[b]	M–K class References
Nov 1993	?	55°	H	Berdyugina et al. (2001b)
Jan 1994	?	55°	H	Berdyugina et al. (2001b)
May 1994	?	55°	H	Berdyugina et al. (2001b)
Jan 1995	?	55°	H	Berdyugina et al. (2001b)
Mar 1995	0.08	65°	P-H, L	Rice and Strassmeier (1998)
May 1995	?	55°	H	Berdyugina et al. (2001b)
Oct 1995	?	55°	H	Berdyugina et al. (2001b)
Dec 1995	…	55°	P, H, L	Donati (1999)
Nov 1996	0.06	65°	H, L	Kővári et al. (2004)
Nov 1996	0.06	65°	H, L	Kővári et al. (2004)
Nov 1996	0.06	65°	H, L	Kővári et al. (2004)
Dec 1996	0.06	65°	H, L	Kővári et al. (2004)
Dec 1996	0.06	65°	H, L	Kővári et al. (2004)
Dec 1996	…	55°	P, L	Donati (1999)
Jan 1998	…	60°	P, H, L	Donati et al. (2003)
Oct 1998	?	55°	H	Berdyugina et al. (2001b)
Jan 1999	…	60°	P, L	Donati et al. (2003)
Mar 1999	?	55°	H	Berdyugina et al. (2001b)
Jun 1999	?	55°	H, L	Berdyugina et al. (2001b)
Dec 1999	…	60°	P, L	Donati et al. (2003)
Apr 2000	0.14	65°	H, L	Kővári et al. (2004)
May 2000	0.14	65°	H, L	Kővári et al. (2004)
Dec 2000	…	60°	P, H, L	Donati et al. (2003)
Dec 2001	…	60°	P, H, L	Donati et al. (2003)
HD283572	WTTS	1.549	78	G5 IV
Feb 1993	0.1	60°	P	Joncour et al. (1994a)
Oct 1997	0.05	35°	P,(L)	Strassmeier and Rice (1998b)
HII 314	Pleiad	1.47	38.7	G1-2V
Nov 1998	…	50°	P, H, L	Rice and Strassmeier (2001)
HD171488	Single	1.337	39.0	G0V
Apr 1998	0.05	55°	P, H, L	Strassmeier et al. (2003b)
Jul 1999	…	60°	P, H	Järvinen et al. (2008)
Sep 1999	…	60°	P, H	Järvinen et al. (2008)
Aug 2001	…	60°	P, H	Järvinen et al. (2008)
Aug 2002	0.08	60°	P, H	Järvinen et al. (2008)
Sep 2004	…	60°	P, H	Marsden et al. (2006)
Jul 2005	…	60°	P, H	Järvinen et al. (2008)
σ^2CrB A	BY Dra	1.157	26	G0V
May 2000	0.02	28°	P, H, Lw	Strassmeier and Rice (2003)

Table 2 continued

Star Epoch	Type[a] ΔV	$P_{\rm rot}$ i	$v \sin i$ Spots[b]	M–K class References
σ^2CrB B	BY Dra	1.157	26	F9V
May 2000	0.02	28°	P, H, Lw	Strassmeier and Rice (2003)
PZ Tel	WTTS	0.94	68	K0V-IV
Jul 1998	…	65°	P, H	Barnes et al. (2000)
YY Gem A	BY Dra	0.8143	48	dM1e
Feb 1993	…	87°	H, L	Hatzes (1995c)
YY Gem B	BY Dra	0.8143	48	dM1e
Feb 1993	…	87°	H,(L)	Hatzes (1995c)
LW Hya	CBPN	0.763	90	wd + G8III-IV
May 1998	0.04	45°	H	Unruh et al. (2001)
AP 193	αPer	0.748	64	G5-6V
Dec 1998	…	55°	H	Barnes et al. (2001b)
ER Vul A	BY Dra	0.698	85	G0 V
Jul 1992	yes	67°		Piskunov et al. (2001)
Jun 1993	…	67°	H, L,Lw	Piskunov (1996)
Aug 1994	yes	67°		Piskunov et al. (2001)
Jul 1994	yes	67°		Piskunov et al. (2001)
Jul 1996	yes	67°		Piskunov et al. (2001)
ER Vul B	BY Dra	0.698	85	G5 V
Jul 1992	yes	67°		Piskunov et al. (2001)
Jun 1993	…	67°	H, L,Lw	Piskunov (1996)
Aug 1994	yes	67°		Piskunov et al. (2001)
Jul 1994	yes	67°		Piskunov et al. (2001)
Jul 1996	yes	67°		Piskunov et al. (2001)
BV Cen	CV	0.6112	93.5	G5-8 IV/V
Jul 2004	0.15	53°	P, H, L	Watson et al. (2007a)
He 520	αPer	0.6038	89	G6V
Nov 1996	0.11	65°	P, H, L	Barnes et al. (2001b)
SV Cam	RS CVn	0.59	117	G2V-IV
1993-1994	0.07	90°	H, L	Hempelmann et al. (1995)
HD307938	Single	0.5641	92	G2V
Jan 2000	0.04	60°	P, H, L	Marsden et al. (2005)
Mar 2003	…	60°	P, H, L	Marsden et al. (2004)
TWA 6	WTTS	0.5409	72	K7
Feb 2006	…	47°	P, H, L	Skelly et al. (2008)
Feb 2006	…	47°	P, H, L	Skelly et al. (2008)
V471 Tau	Pre-CV	0.5211	89.5	K2V
Sep 1992	…	90°	P, H, L	Ramseyer et al. (1995)
Oct 1992	…	90°	P, H	Ramseyer et al. (1995)
Dec 1992	…	90°	P, H, L	Ramseyer et al. (1995)

Table 2 continued

Star Epoch	Type[a] ΔV	P_{rot} i	$v \sin i$ Spots[b]	M–K class References
Dec 1993	0.1	90°	P, H	Ramseyer et al. (1995)
Nov 2002	…	80°	P, H	Hussain et al. (2006)
Nov 2002	…	80°	P, H	Hussain et al. (2006)
AB Dor	Single	0.5148	89	K0 V
Feb 1989	0.1	60°	H, L	Kürster et al. (1994)
Jan 1992	…	60°	P, H, L	Collier Cameron and Unruh (1994)
Dec 1992	…	60°	P, H, L	Collier Cameron (1995)
Nov 1993	0.15	60°	P, H, L	Unruh et al. (1995)
Nov 1993	0.15	60°	P, H, L	Unruh and Collier Cameron (1997)
Nov 1993	0.15	60°	P, H, L	Hussain et al. (1997)
Nov 1994	0.13	60°	P, H, L	Collier Cameron et al. (1999)
Dec 1995	…	60°	P, H, L	Donati and Collier Cameron (1997)
Dec 1996	…	60°	P, H, L	Donati et al. (1999)
Jan 1998	…	60°	P, H, L	Donati et al. (2003)
Jan 1999	…	60°	P, H, L	Donati et al. (2003)
Dec 1999	…	60°	P, H, L	Donati et al. (2003)
Dec 2000	…	60°	P, H, L	Donati et al. (2003)
Dec 2001	…	60°	P, H, L	Donati et al. (2003)
He 699	αPer	0.4908	93.5	G2-3V
Oct 1996	0.10	52°	P, H	Barnes et al. (2001b)
Nov 1996	0.12	52°	P, H	Barnes et al. (2001b)
Oct 2000	0.05	52°	P, H	Jeffers et al. (2002)
EY Dra	Single	0.4586	62	M1-2V
Jun 1996	…	70°	P, H, L	Barnes et al. (2001)
V374 Peg	Single	0.4456	36.5	M4V
Aug 2005	…	70°	H, L	Donati et al. (2006a,b)
Sep 2005	…	70°	H, L	Morin et al. (2008)
Aug 2006	…	70°	H, L	Morin et al. (2008)
MN Lup	CTTS	0.439	74.6	M0
May 2000	0.10	46°	L	Strassmeier et al. (2005)
May 2000	0.10	46°	L	Strassmeier et al. (2005)
HK Aqr	Single	0.4307	69	M1.5V
Aug 1991	…	90°	L	Barnes and Collier Cameron (2001)
LO Peg	Single	0.4236	65	K5-7 V
Aug 1993	…	35°	P, H, L	Lister et al. (1999)
Jul 1998	…	45°	P, H	Barnes et al. (2005)
Sep 2003	…	45°	P, H	Piluso et al. (2008)
HII 3163	Pleiad	0.418	70	K0V
Dec 1993	0.2	58°	P, H, L	Stout-Batalha and Vogt (1999)
AE Aqr	CV	0.4116	100?	K3-5 V/IV

Table 2 continued

Star Epoch	Type[a] ΔV	$P_{\rm rot}$ i	$v \sin i$ Spots[b]	M–K class References
Aug 2001	0.15	66°	H, L	Watson et al. (2006)
HII 686	Pleiad	0.397	64	K4V
Dec 1993	0.11	51°	P, H, L	Stout-Batalha and Vogt (1999)
HD197890	WTTS	0.380	132	K3V
Jul 1998	…	55°	H, L	Barnes et al. (2001a)
Jul 2002	…	70°	P-H	Barnes (2005)
Aug 2002	0.05	70°	H, L	Wolter et al. (2005)
Aug 2002	0.05	70°	H, L	Wolter et al. (2005)
Oct 2006	0.1	70°	H	Wolter et al. (2008)
AE Phe A	W UMa	0.3624	145	G0V
Nov 1989	…	88°	H, L	Maceroni et al. (1994)
Nov 1990	yes	87°	H, L	Maceroni et al. (1994)
AE Phe B	W UMa	0.3624	95	F8V
Nov 1989	…	88°	H, L	Maceroni et al. (1994)
Nov 1990	yes	87°	H, L	Maceroni et al. (1994)
AP 149	αPer	0.3200	102	G8V
Dec 1998	…	30°	P, H	Barnes et al. (2001b)
YY Eri A	W UMa	0.3125	160	G9V
Nov 1989	…	82°	H, L	Maceroni et al. (1994)
Nov 1990	yes	82°	H, L	Maceroni et al. (1994)
YY Eri B	W UMa	0.3125	110	G7V
Nov 1989	…	82°	H, L	Maceroni et al. (1994)
Nov 1990	yes	82°	H, L	Maceroni et al. (1994)
RXJ1508.6	Single	0.31	115	G2V-IV
May 1998	…	28°	P, H, L	Donati et al. (2000)
V426 Oph	CV	0.2854	?	?
? 2005	…	63°	H, L	Watson et al. (2007b)
VXR45A	Single	(0.176)	238	G9V
Mar 2003	…	?	P, H, L	Marsden et al. (2004)

The order is according to decreasing rotational period, $P_{\rm rot}$, in days. "Type" denotes the variable-star type of the target (see end of table for a detailed listing), ΔV is the amplitude of the V-band light at the time when the Doppler image was taken and an entry also means that photometry was used as additional input for the mapping (dots in this column mean that no light-curve information was used for the Doppler image), i is the inclination of the rotational axis adopted by the various authors, $v \sin i$ is the projected rotational velocity in km s^{-1}, "Spots" gives a brief indication of the surface location of spots recovered (see end of the table for a listing of the acronyms), "MK-class" is the Morgan–Keenan classification of the stellar spectrum

[a] RS CVn = close binary with evolved component(s); BY Dra = close binary with main-sequence components; WTTS = weak-lined T Tauri star; CTTS = classical T Tauri star; CBPN = central binary of planetary nebula; W UMA = contact binary; FK Com = single rapidly rotating giant; Eff.-single = effectively single star (but component in wide binary); Pleiad = member of Pleiades cluster, single star; α-Per = member of α-Per cluster, CV = cool secondary in a Cataclysmic Variable; Single = single star, unspecified

[b] P = polar spot, H = high-latitude spots, L = low-latitude spots (w = warm spot relative to the effective temperature)

homepage[2] and supersedes the table in Strassmeier (2002). It lists the month and year of observation, the variable-star type, the star's M–K classification, the rotational period and the rotational velocity, the amplitude of the V-band light curve in case this information is used for the image recovery, the inclination of the stellar rotation axis and whether a polar spot (P), or high-latitude (H), or low-latitude (L) spots were present.

The 79 individual stars in Table 1 consist of 38 single or effectively single stars and 41 components in close binary systems. The sample includes one effectively single giant (CM Cam), which is a component in a wide visual binary with a 10-year orbit and two stars which are the late-type companions of a central star of a planetary nebula (IN Com and LW Hya). Four further entries are the components of two contact binaries (AE Phe and YY Eri), and three entries are the cool components of cataclysmic variables (CV) (AE Aqr, BV Cen, and V426 Oph). V471 Tau has been classified as a pre-CV binary because it has a white dwarf as the hot component but does not show the significant outburst and mass transfer signatures. Five more entries are double-lined close binaries where both components have a Doppler image (TY Pyx, V824 Ara, σ^2 CrB, YY Gem, and ER Vul) and one star recently even a Zeeman–Doppler image (V824 Ara = HD155555; Dunstone et al. 2008).

Dark spots on W UMa-type systems[3] were first proposed by Binnendijk (1970) to explain the asymmetric eclipses in some systems and Mullan (1975) followed up with a more detailed investigation. The first Doppler maps were obtained for VW Cephei by Hendry and Mochnacki (2000) from data taken from 1991 to 1993. Spots covered 66% of the surface of the primary and 55% of the secondary mostly at the rotational poles, much more than that detected for non-contact binary stars and over-active single stars. However, a large number of non-black spots must have coexisted in VW Cep because the bolometric flux-weighted mean surface temperature of the primary turned out to be less than that of the secondary. This indicated a great number of unresolved spots. W UMa spectra are notoriously difficult to analyse due to their immense line broadening and the double-lined nature as well as being relatively faint. Therefore, they appear underrepresented in Tables 1 and 2 despite of their heavy spottedness.

9 Spot sizes

This is a controversial issue because the current results are still dependent on the techniques and assumptions applied. Also, it is to be defined what spot "size" or "area" really means. As seen from white-light images of the Sun, sunspots contrast very sharply and spot area is easy to determine while (Doppler) images appear much smoother and are of comparably poor resolution, sometimes even "pixelized". The smoothness could be real or an artefact due to finite integration time or the choice of

[2] http://www.aip.de/groups/activity.

[3] W Ursa Majoris systems are very close binaries in a common outer envelope, usually convective. Their surfaces are distorted along the apsidal line by the respective gravitational pull and oblate due to their fast rotation. All W UMa systems appear as eclipsing binaries.

the regularization algorithm (by definition Maximum Entropy favours a sharper representation while Tikhonov favours a smoother representation; see Piskunov 1991). If the data are good this information is preserved in a spectral line profile and, in principle, can be reconstructed properly. However, spots are likely constantly changing, just like sunspots, so that even if different mapping techniques are applied to the same star the data must be taken at the same time to make a meaningful technical comparison (likely still not conclusive though). So, it is helpful for this review to reconsider the various mapping techniques and their constraints on spot areas.

Temperature Doppler imaging inverts a time series of spectral line profiles with well-known atomic parameters into a surface temperature map. It requires knowledge of the local line profile of the (unspotted and spotted) stellar photosphere. It is usually computed from a radiation-transfer solution through an LTE model atmosphere for the adopted atomic line parameters of the line(s) in question. For the inversion process every surface pixel is then assigned a "temperature". Note that the temperature information is preserved through the excitation potential of the (neutral) line which, to first order, marks its temperature sensitivity. Then, it greatly helps if the neighbouring continuum is also included in the inversion, e.g. through broad- or intermediate-band photometry (e.g. Rice 2002). The reconstructed size of a spot should be independent of the temperature sensitivity of the spectral line but if all the line's atomic parameters are known just slightly inaccurately cross talk between, say, temperature sensitivity and transition probability may result in inaccurate images. Moreover, if the flux-tube bundle picture (Parker 1955) also applies to starspots, the reconstructed spot size would intrinsically depend on the height of origin in the atmosphere where the spectral line is formed (to first order also on the strength of the line as long as it is optically thin). Then, in principle, we expect to obtain different spot sizes for strong and weak spectral lines, respectively.

Brightness (*or spot-filling factor*) *Doppler mapping* makes use of only the information from the observed line-profile shape (while temperature mapping implicitly also uses the line equivalent width). For the inversion process every surface pixel is assigned a dimensionless "intensity" or a "filling factor" that can be converted to brightness by simple disk integration with proper aspect-angle weighting. Figure 4 shows an example of two Doppler images of the same star, obtained independently at approximately the same time by two different groups with two different codes, one with temperature mapping with photometry (Rice and Strassmeier 1996) and the other with spot-filling-factor mapping and without photometry (Hatzes 1995). It shows remarkable similarity despite that the reconstructions were done even with different inclination of the rotational axis (70° vs. 54°). The most differences are in contrast and these differences are largely due to the incorporation of photometric data. Including photometry improves the reconstruction in the image of the global temperature variations. The reconstructed spot sizes are now primarily limited by their definition, i.e. where does a spot end and the undisturbed photosphere begin.

Many Doppler-imaging reconstructions of starspots and surface magnetic fields now in the literature were obtained by assuming a two-temperature structure on the stellar surface (Collier Cameron 1992; Vogt et al. 1999; Donati et al. 2006a,b), i.e. the reconstructed images resemble white-light images of the Sun but with only two temperatures allowed. One temperature is set to be the photospheric temperature, the other

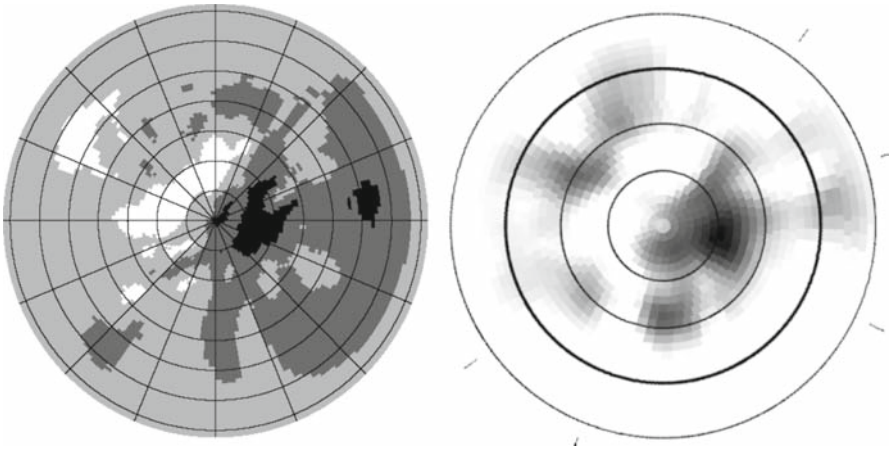

Fig. 4 A comparison of two images of the weak-lined T Tauri star V410 Tau obtained by two groups independently at the same time. The projections are "pole on". The stellar equator is indicated as a *thick circle*. The *left* image was obtained by Rice and Strassmeier (1996) at CFHT including photometry, the *right* image was obtained by Hatzes (1995) at McDonald Observatory without photometry. Inspite of fact that the reconstruction was done with different assumptions of the inclination of the rotational axis and with different inversion codes, the two images appear encouragingly similar. Figure from Rice (2002)

is the spot temperature. The reconstruction then generates a "thresholded" brightness image because the inversion process suppresses any other temperature. It is debatable (e.g. Hendry and Mochnacki 2000) whether this thresholding or the introduction of bright regions is a more realistic approach to fit the line profiles to the full extent of the S/N of the data. Uniform spot temperatures make the determination of spot sizes easier but also more model dependent. The interpretability even worsens when an average line profile is used for the image reconstruction, like, e.g. in least-squares-deconvolution (LSD) profiles (Semel 1989; Donati et al. 1997). Such profiles can be mean Stokes I (intensity) or Stokes V (circular polarized) line profiles extracted from hundreds or even thousands of lines from an echelle spectrum. LSD can create a mean line profile with a superior S/N ratio of even thousand to one but assumes that starspots affect all rotationally broadened lines in the same way. This assumption is the better fulfilled the higher the rotational broadening and thus the more independent the inversion is of the knowledge of the local line profile. A variant of LSD, dubbed "selective LSD" by Wolter et al. (2005), is less prone to above assumption because it is applied to a selected, narrower, wavelength range. True spot areas from LSD or sLSD images of slowly rotating stars have to be taken with care, particularly when comparing to, say, temperature maps. A new technique based on a principal component analysis (PCA) that bypasses most of the shortcomings of LSD has recently been presented and applied (Rámirez Velez et al. 2006; Carroll et al. 2007; Martinez González et al. 2008). Its kernel features a decomposition of n spectral line profiles into its eigenvectors and then cross-correlates all eigenvectors with the profile of a selected, particularly well-suited line profile, which then allows the reconstruction of this particular profile using the cross-correlation function from the n other lines.

Thereby, S/N can be increased by one or maybe two orders of magnitude just by selecting a suite of appropriate input profiles; e.g. with 18 input profiles from a wavelength range between 460 and 660 nm, Carroll et al. (2007) achieved an increase of S/N in Stokes V of FeI 549.7 nm of roughly a factor of ten. Moreover, the major advantage of this approach as compared to LSD or sLSD is that wavelength space is preserved and thus allows to apply a full radiative-transfer treatment during the line-profile inversion process.

Nevertheless, the Doppler images summarized in Table 2 show starspots with a size range between 22% of a hemisphere (XX Tri, see below) and the target-dependent detection limit of, say, a tenth of a per cent. True polar cap-like spots are not counted here because their size determination is notoriously uncertain due to the absence of (or almost absent) Doppler signal. Note that the sunspots typically cover 10^{-4} to 10^{-5} of the solar surface and only during solar maximum reach about 10^{-3}. The record holder is still the one big starspot seen in a Doppler image of the active K giant XX Tri in December 1997 (Strassmeier 1999, Fig. 5). Based on the star's Hipparcos distance of 197pc the spot's size is approximately 11 million km ($\sim 12 \times 20$ solar radii), i.e., 60 times the extension of the largest ever observed sunspot group or 10,000 times its areal coverage. Such dimensions may have an impact on the local hydrostatic equilibrium because a sunspot-like Wilson depression[4] would make the star look like the logo of a well-known computer company.

The smallest spots are detected on those stars that exhibit the largest ratio of the local line broadening to the stellar rotational line broadening because then the Doppler resolution on the stellar surface is the highest (see, e.g. Collier Cameron 1992). Isolated spots of $10^\circ \times 10^\circ$($\approx$0.15% of the surface) were detected on the ultra-rapidly rotating K3 dwarf Speedy Mic = BO Mic (Barnes 2005; Wolter et al. 2005), having a $v \sin i$ of 132 km/s and a rotation period of 0.38 days.

Solanki and Unruh (2004) explore the consequences if starspot areas were distributed just as sunspot areas, i.e., show a log-normal size distribution throughout the activity cycle (which implies that most sunspots are small). From an extrapolation to higher activity levels, as appropriate for active stars within reach of the Doppler-imaging technique, they proposed that, even for heavily spotted (hypothetical) stars, a large fraction of the spots are smaller than the current resolution limit of Doppler images and hence might be missed by traditional Doppler maps. One way out may be the incorporation of molecular lines into the inversion process as suggested by O'Neal et al. (1996, 2004) and incorporated by Berdyugina (2002), Savanov and Strassmeier (2005) and Rice (2008, private commun.) but not yet applied to full extent to real stars[5] because of a lack of proper infrared spectra and accurate molecular laboratory data.

[4] I.e. a depression in the optical-depth unity ($\tau = 1$) surface due to the lower gas temperature, density and pressure in the presence of a magnetic field with respect to the field-free surrounding. The depression is approximately 500–700 km for a small Sunspot (cf. Loughhead and Bray 1958).

[5] Recently, Berdyugina (2009) presented a first 3D-Doppler image from optical molecular band inversions of the M dwarf AU Mic.

10 Spot temperatures

As long as we have just one-dimensional data, i.e. rotational light curves, the determination of a starspot temperature is always mathematically correlated with the determination of the starspot size. Early attempts to disentangle these two quantities (e.g. Poe and Eaton 1985) were based on the inclusion of colour variations (usually $V–I$ for late-type stars) simultaneous with brightness variations (usually Johnson V). However, colour curves are still one-dimensional data and the temperature extraction accordingly uncertain. A standard approach is to iteratively solve for spot area and temperature from V and $V–I$ curves (e.g. Oláh and Strassmeier 1992). The relative error can be rather small ($\pm$100 K) but sometimes it is of the same order as the temperature difference between the photosphere and the spot itself (see, e.g. Eker 1999).

Not all Doppler imaging inversion codes can provide an absolute spot temperature because of the choice of the inversion parameter in their coding. A temperature Doppler imaging code requires a full radiative-transfer analysis for the local line profile for the full range of surface temperatures, chemical abundances, and limb angles. The light-curve inversions are more prone to global uncertainties than local uncertainties and require high-precision, absolutely calibrated, multi-bandpass photometric data, at least either $V–R$ or $V–I$ (spot temperatures from $B–V$ are debatable because of a possible plage contribution to B). Some studies actually simultaneously incorporate the inversion of both data type, spectroscopy and photometry, and these are likely the sources with the best determined spot temperatures. For evolved stars, photometric zero points are notoriously uncertain (e.g. Kaiser et al. 2007) and an absolute all-sky calibration often introduces an uncertainty of the order of the photometric amplitude of the star itself. Therefore, mostly just differential photometry is being used in the line-profile inversion with a few exceptions for dwarf stars (e.g. for EK Dra as shown in Fig. 1). Absolute spot temperatures are therefore still rare and sometimes inconsistent when using different techniques.

Gray and Johanson (1991) have shown that line-depth ratios provide an alternative tool for spot temperature determination with the advantage that they are best measurable for very slowly rotating stars, where Doppler imaging fails. Precisions in relative temperature of less than 10 K were achieved for selected stars. The technique relies on a pair of closely spaced, unblended and unsaturated spectral lines where one line is temperature-sensitive and the other not. If a cool spot is in sight on the stellar disk then the temperature-sensitive line will increase in strength while the temperature-insensitive line will remain more or less unaffected. Strassmeier and Schordan (2000) and Gray and Brown (2001) provided a calibration for giant-star spectra and Catalano et al. (2002) combined the line-depth ratio technique with simultaneous photometry and then were able to disentangle the spot area from the spot temperature. For three particularly active RS CVn stars, VY Ari, IM Peg, and HK Lac, Catalano et al. (2002) derived spot temperatures cooler than the photosphere of $\Delta T = T_{\rm phot} - T_{\rm spot} \approx$ 720–980 K with a spot-to-photosphere ratio ($T_{\rm spot}/T_{\rm phot}$) of around 0.8. Comparable values of $T_{\rm spot}/T_{\rm phot} \approx 0.8$ were subsequently found for II Peg and λ And (Frasca et al. 2008). Two groups, Frasca et al. (2008) from line-depth ratios and O'Neal et al. (1996) from TiO spectrum fitting, independently found a weak tendency of increased ΔT with gravity which could be explained by the increased magnetic pressure inside

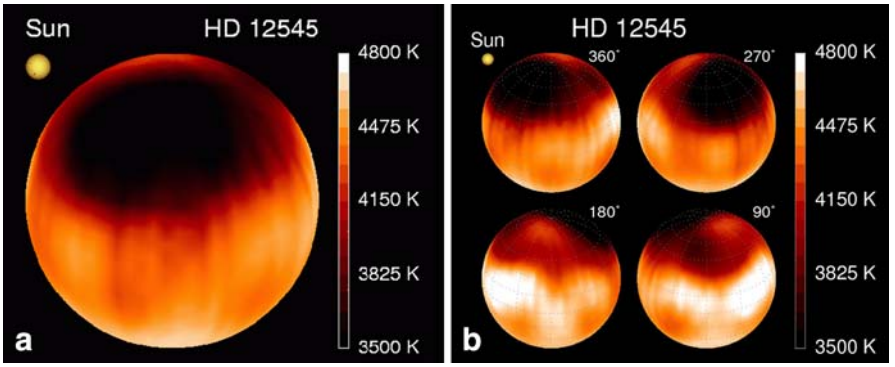

Fig. 5 **a** The gigantic starspot (*black region*) of the K giant XX Tri = HD12545. Shown is a Doppler image in spherical projection with surface temperature as labelled. For comparison, the plot shows a white-light image of the Sun at a time when the largest ever observed sunspot group was visible on its surface (note that the Sun is plotted on the same scale as XX Tri). The spot on XX Tri is about 10,000 times larger than this sunspot group and had a temperature cooler by $1,300 \pm 120$ K with respect to the undisturbed photosphere. **b** The same Doppler image but shown at four different rotational phases as indicated. Surprisingly, the hemisphere opposite to the big cool high-latitude starspot shows an elongated bright equatorial feature with a temperature warmer by ≈350 K. Together with the cool superspot it caused the record V light-curve amplitude of 0.63 mag. We note that these data were obtained with the smallest telescope on Kitt Peak, the now retired 0.9 m coudé feed telescope (Strassmeier 1999)

a flux tube that is needed to balance the higher external gas pressure in the higher gravity stars. More data are needed in order to make the current results fully conclusive. Berdyugina (2005) also showed that, on average, ΔT appears larger for hotter stars with values near 2,000 K for the late F and early G stars dropping to 200 K for the late M stars. This appears to be the case for any gravity but, again, the sample is rather inhomogeneous and not large enough yet to be conclusive, particularly not for the M stars. Spot temperatures from both photometry and Doppler imaging were recently collected from the literature and presented by Berdyugina (2005) and I refer to her table.

Chapman et al. (2003) found a (still debated) correlation between sunspot darkness and sunspot size while Albregtsen and Maltby (1978) had found a (also debated) correlation of sunspot darkness with sunspot cycle (see Stix 2002 for a more detailed discussion and other references). For starspots, there seems to exist no strong correlation between temperature and size for any of the types of variable stars or evolutionary status (Bouvier and Bertout 1989; Strassmeier 1992). The large range of spot temperatures and sizes is probably the only significant finding. For sunspots, Parker (1979) showed that young spots must emit MHD waves which should cool them within 3 min (the time for the energy to cross the spot) while solar observations (e.g. Chou 1987) reveal cooling times between 0.5 and 9 h, i.e. a factor of 10–100 longer than predicted. Starspots can be larger than sunspots by many factors, in the extreme case even up to a factor of 10,000 as shown in Fig. 5, and their respective cooling times should be even substantially longer than for sunspots. Therefore, one and the same starspot could have been observed at quite different temperature if its lifetime is just long enough, which would suggest that the observed large range of starspot temperatures is a simple

selection effect. This appears to be the case, e.g. for AR Lac with $T_{\rm spot} = 1,320 \pm 590$ K in 1978 and 230 ± 180 K in 1981 (Kang and Wilson 1989).

11 Spot (and plage) cycles and polar spots

Lockwood et al. (2004, 2007) presented clear evidence that a relation between photospheric and chromospheric cycles exists. For the older stars in the Mt. Wilson Observatory (MWO)-survey sample, e.g. HD 10467 (K1V), the relation is solar-like, i.e. the photospheric brightness varies in phase with the chromospheric brightness (the Sun becomes brighter when it is more active and covered with more spots due to the dominating plage component). For the "young" stars, e.g. HD 1835 (G2.5V), a predominantly anti-solar behaviour is seen, i.e. the photosphere varying inversely in phase with the chromosphere. This reinforces our presumption that stellar photospheric and chromospheric cycles are due to the cyclic appearance of starspots and plages, respectively.

Also thanks to the late MWO-survey (e.g. Wilson 1968), we now know about 30 stars with long-term chromospheric magnetic activity cycles in the period range 3–21 years (Baliunas et al. 1995; Frick et al. 2004; Lockwood et al. 2007). Another roughly one-third of the $\approx$ 100 stars with such long-term data exhibit no cycle at all and have rather low average CaII H&K emission. These stars comprise a very interesting subgroup from a dynamo perspective. Another group are the ones that exhibit a single cycle period but either with a constant amplitude or with a grossly different amplitude from cycle to cycle. A third group is stars where the observations strongly suggest the existence of a cycle but with a period that is longer than the current interval of observation. A fourth group is stars with double-periodic cycles. Finally, a fifth group consist of stars that clearly show variations but no period is detectable.

Photospheric cycles were first recognized by Phillips and Hartmann (1978) who presented long-term photometry based on scans of photographic magnitudes from archival plate collections. They found a 50–60-year variation for BY Dra and CC Eri, two spotted dwarf stars. A comparable value was published by Hartmann et al. (1981) for V833 Tau = BD + 26°730, a K5 dwarf in a single-lined BY Dra-type binary.[6] V833 Tau is still the coolest star known to exhibit a clear photospheric cycle, with a 71-year period (originally from Oláh et al. 2001 but revised in Strassmeier 2005 with more data). The coolest stars with a chromospheric (H&K) cycle seem to be 61 Cyg B (K7V) with a cycle period of 11.7 years and its visual companion 61 Cyg A (K5V) with a cycle period of 7.3 years (Baliunas et al. 1995). Both periods are significantly shorter than the photospheric cycle lengths of other similar stars obtained from archival plates. ROSAT X-ray observations of both 61-Cyg components revealed a trend that appeared in phase with the respective H&K cycle. Hempelmann et al. (2003) concluded that the X-ray emission is likely cyclic with the same period as the H&K emission. However, no photospheric cycle has been reported for 61 Cyg yet. Note that the M2 dwarf GJ 411 is the coolest star in the entire MWO sample and Baliunas et al. (1995) reported on its CaII H&K variability but found no cycle period. High-precision

[6] BY Draconis binaries are active close binaries that contain two low-mass main-sequence stars.

APT photometry[7] during two observing seasons revealed no photometric variability above ≈1 mmag, and clearly no photometric cycle (Henry et al. 2000).

Collecting most of the available literature data at that time, Saar and Brandenburg (1999, 2002) likely found evidence of a non-linear dependency of fractional cycle amplitude, i.e. the ratio of the peak-to-peak variation to the average, with $B–V$ colour in the sense that the H&K-cycle amplitude is larger in early to-mid K stars than in G and F stars. It even drops significantly after mid K (no M star has yet a cycle observed). This behaviour suggests some sort of connection of a cycle with the fractional depth of the convection envelope, which affects photospheric tracers of magnetic fields more than chromospheric (H&K) and coronal (X-rays) ones. For K to F main-sequence stars, it is generally agreed that the convection envelope becomes thinner the higher the effective temperature and, at least according to mean-field dynamo theory, a connection to the cycle amplitude is not surprising. But for the low-mass stars cooler than, say, mid K to early M, this trend likely breaks down, possibly due to a thinner and thinner and eventually absent tachocline and the resulting turbulent dynamo. These stars' convective envelope may be so deep that its resulting dynamo pattern disconnects from the surface, or at least makes the connection not so obvious as for the tachocline stars (see also Fig. 14). In this respect it is not surprising that inferred radii from eclipsing early M dwarfs appear to be 10–20% larger than what all current stellar-structure models predict (see, e.g. Morales et al. 2008, 2009).

From 35 years of photographic plates, Fröhlich et al. (2002) found a secular B-magnitude dimming of a true solar-type star (EK Dra = HD129333) beginning in around 1975 in agreement with contemporaneous photoelectric APT data, but found no cycle period. Messina and Guinan (2002) found a 9.2 years V-brightness cycle with additional evidence for a long-term trend of more than 30 years for that very same star. There is also evidence that the starspot minimum in 1994/1995 coincided with the lowest X-ray flux observed so far (Güdel et al. 2003). Recently, Järvinen et al. (2005) analysed 21 years of photoelectric data of EK Dra and confirmed the existence of a V-band photometric cycle but with a slightly longer period of 10.5 years. They also concluded that the overall brightness of the star had been decreasing for at least 45 years, as found earlier by Fröhlich et al. (2002). If also due to starspots and not, e.g. due to a decreasing plage or network contribution, we may speculate that the star accumulated cool starspots around the rotational poles, at least on the one pole that is always in view for observers, that then decay and fade away until new magnetic flux was added. This is part of a picture put forward by Schrijver and Title (2001) based on heliograms, but evolved for an artificially spun-up Sun. Indeed, a first Doppler image of EK Dra (Strassmeier and Rice 1998a,b) had shown a significant high-latitude spot (cf. Fig. 1), although not a polar cap as in many RS CVn binaries (see Table 2). Therefore, we would expect that very high-latitude starspots once developed into a polar cap-like feature do not anymore participate in the cyclic behaviour of their lower latitude precursors and, indeed, no such variations have been found and claimed for any active star so far. E.g. 11 years of almost continuous Doppler imaging of the G5 subgiant EI Eri (Washuettl et al. 2008; see also Strassmeier

[7] Automatic Photoelectric Telescopes, see http://www.fairobs.org.

2005) revealed no significant areal changes of its huge cap-like polar spot, neither did the observations by Vogt et al. (1999), Strassmeier and Bartus (2000) or Petit et al. (2004a), Petit et al. (2004b) for HR 1099. For AB Dor, however, the very first Doppler images obtained in 1988 and 1989 showed no polar cap at all, just high-latitude spots, but a polar cap-like spot was reconstructed in all subsequent Doppler images (Jeffers et al. 2007, but see also Hussain 2002 and references therein). Note that AB Dor was at its minimum brightness in 1988, i.e. likely maximum spottedness, and has been increasing in brightness ever since. In spite of this opposite behaviour compared to EI Eri and HR 1099, it still supports the picture of magnetic flux swept to and accumulated at the poles. Also, AB Dor is a single ZAMS star (although with a wide visual binary component) while EI Eri and HR1099 are evolved components in close binaries.

For another spotted star, the active K1 giant HK Lac, Oláh et al. (2000) had already collected 30 years of photoelectric data that were supplemented by 35 years of archival plate magnitudes by Fröhlich et al. (2005), resulting in a 46-year-long photometric database with roughly 20 years of overlapping data. Both data sets independently showed a 13.0- and a 6.8–7.0-year period, while the plate magnitudes had yet another period of 9.2 years in the power spectrum. Note that these plate data are relatively precise and even revealed the 24.4-day rotational period of the star and thereby prove their surprisingly good quality. Also note that the Doppler images of HK Lac by Weber et al. (2001) showed no cap-like polar spot but only high-latitude and low-latitude spots. HK Lac maybe just a counter example to EI Eri, HR 1099, and AB Dor, and others in the zoo, or the star was just caught in a long-lasting phase of global spot reorganization.

Recently, Oláh and Strassmeier (2007); Oláh et al. (2009) applied the short-term Fourier transform time-frequency analysis to a sample of 21 stars, including the Sun, and discovered either a systematic increase, or a decrease, of one or both of the cycle periods for three active binaries (HR1099, IL Hya, HK Lac) and one lower main-sequence single star (HD 100180). For comparison, the 200-year-long sunspot number record was used exactly the same way and suggested a decreasing Schwabe-cycle[8] period (from $\approx$11.1 to 10 years). It also verified the currently increasing Gleissberg-cycle[9] period claimed earlier by Oláh and Strassmeier (2002) from 500 years of sunspot data collected and prepared by Kolláth (Kolláth and Oláh 2009). From another, though preliminary, analysis of 385 years of sunspot data, Rogers et al. (2006) identified a period of 188 ± 38 years (with weaker periods of $\approx$40 and 87 years), possibly related to the basic Schwabe cycle. They noticed a correlation between the times of historic minima and the length of the sunspot cycle such that the length of the cycle was usually highest when the actual number of sunspots was lowest. While the solar and the stellar data are not yet directly comparable, it appears that changing multi-period cycles like on the Sun are common also among spotted stars. We note that stars with polar spots in the sample of Oláh et al. (2009) show cycle variations

[8] The Schwabe cycle is the Sun's most dominant activity cycle, usually called the 11-year sunspot cycle.

[9] The Gleissberg cycle is around 80 years and modulates the Schwabe cycle (e.g., Gleissberg 1958). Its period remains within 6 and 7 Jovian years. The cosmogenic isotope record provided by ^{14}C extends back to 11,600 years and suggests an average cycle period of 87.8 years with time-dependent variations (Peristykh and Damon 2003).

comparable to the ones without a polar spot. We could interpret this such that only the equatorial or low-latitude spots appear and disappear in a cyclic manner, while the polar spots follow another time scale.

12 Activity "flip–flops"

Flip–flops are a comparably unexplored phenomenon and were first noticed from light-curve phase jumps of the spotted giant star FK Comae (Jetsu et al. 1991). These are explained with the existence of two active longitudes (phases) 180° apart with alternating levels of spot activity (Korhonen et al. 2001). Stars with long enough data baselines even show a back and forth ("flip and flop") of the activity within these two longitudes. The average time between such flip–flops is also referred to as a flip–flop cycle and has been observed to be in the range of a few years up to a decade. An observational overview and an inventory of stellar targets with such cycles was given recently by Berdyugina (2005, 2007) and Korhonen and Järvinen (2007) and is not repeated here. After its discovery in cool stars, the phenomenon has also been claimed to exist on the Sun (Berdyugina and Usoskin 2003), one of the few examples where the solar–stellar connection provided discovery in the opposite direction.

Moss (2004) and Elstner and Korhonen (2005) presented the first dynamo models based on a combination of a non-axisymmetric dynamo mode with an oscillating axisymmetric mode to explain the phenomenon. Elstner and Korhonen (2005) found stable mixed-mode solutions for weakly differentially rotating stars and succeeded with their numerical simulations in following the cycle for over 100 diffusion times. Under the assumption of a weakly differentially rotating star with a thick convective envelope and overcritical α-effect, Korhonen and Elstner (2005) were able to reproduce the flip–flop period and the high-latitude appearance of the spots on FK Comae. These models predict that a flip always takes place at maximum spottedness, exactly what has been observed, e.g. on HD 291095 (Savanov and Strassmeier 2008) and what was suggested earlier by Fluri and Berdyugina (2004) from their dipole and quadrupole mixed-mode model.

The mixed-mode solutions are a promising approach to the complexity of stellar activity in general. The results presented by Elstner and collaborators are in particular sensitive to the amplitude of differential rotation: the mixed-mode solutions appear only in a small window of differential rotation. A disadvantage of this solutions is that the cycle period is also the period for the flip–flops to occur, which is currently observationally unconfirmed.

13 Starspot lifetimes

Hussain (2002) summarized starspot lifetimes in a more detailed review. Her main conclusions and caveats together with now more up-to-date data suggests that, (i) spots on tidally locked binary systems live longer (months) than spots on single main-sequence stars (weeks), (ii) because polar starspots may be formed differently (likely due to magnetic flux swept up to the rotational poles from lower latitudes by strong poleward meridional flows), their lifetime is likely driven by another physical

mechanism, (iii) spot lifetimes from time-series photometry suggest on average a year-long existence, (iv) active longitude "flip–flops" may terminate a spot's or a group of spots' imprint on a light curve and thus mask the regular decay mechanism. Many results indicate that the maximum lifetime of a large monolithic spot or compact spot group is not determined by its Ohmic decay but possibly limited by the surface shear due to differential rotation and/or simple reconnection with the surrounding. In an earlier study, Hall and Busby (1990) and Hall and Henry (1994) computed upper limits of starspot lifetimes from photometry based on the idea that large starspots will be disrupted by the shear of differential rotation. Applied to the spotted RS CVn binary HR7275, Strassmeier et al. (1994a,b) traced 20 individual spots or spot groups and found individual spot lifetimes of up to 4.5 years with an average lifetime of 2.2 years, which was then used to set an upper limit to the differential surface rotation of five to eight times less than solar. On the contrary, Brown et al. (2003) had excluded shear due to differential rotation on the Sun as the cause for the existence of spinning sunspots (see also next section on velocity fields).

If the decay of an isolated sunspot is set by the amount of the azimuthal electric current within the spot which reduces its electric conductivity, a constant area decay would result (see Stix 2002). From a statistical analysis of sunspot data, Petrovay and Van Driel-Gesztelyi (1997) found that an "idealized" sunspot follows a mean decay law of the form $D_{\rm ideal} = C_{\rm D} r/r_0$ with $C_{\rm D} = 32.0 \pm 0.26$, where $D_{\rm ideal}$ is the area decay rate in units of one-millionth solar hemisphere per day, r is the equivalent radius of the spot (the radius of the circle with the same area), and r_0 is its maximal equivalent radius. This implies a parabolic area decay rather than a linear one. Previous observations had shown both linear and non-linear decays (see Martínez Pillet et al. 1993). The systematic deviations from a strict parabolic law were explained by Petrovay et al. (1999) with a generalization of the turbulent erosion model of sunspot decay when flux tubes are embedded in a pre-existing homogeneous plage field. It is worth noting that the theoretical decay rate from 2-D modelling of a sunspot turned out to be close to linear for both the spot area and the magnetic flux (Rüdiger and Kitchatinov 2000). This confusing situation may partly be resolvable with new high-resolution solar observing techniques and instruments and, in addition, by comparing to starspots.

Observations of an isolated starspot from Doppler imaging as a function of time with high sampling are not yet available and again we must also rely on "averaged" or "idealized" starspots. I emphasize that an observation of a starspot decay could place some constraints on the magnetic diffusivity, which itself is a very sensitive parameter for the magnetic-cycle period. Numerical values for the magnetic diffusivity are not known and adopted values range from $10^{10}\,{\rm cm}^2/{\rm s}$ (Dikpati and Charbonneau 1999) to $10^{13}\,{\rm cm}^2/{\rm s}$ (Rüdiger and Kitchatinov 2000). See also Hathaway and Choudhary (2008) for a more recent value of $10^{11}\,{\rm cm}^2/{\rm s}$. This value may also appear to be important for dynamo models that are tailored to predict the next solar activity cycle (Dikpati et al. 2007; but see also Cameron and Schüssler 2007).

Figure 6 is one of the few examples of high-cadence time-series Doppler imaging of a spotted star and shows the continuous growth of a large starspot over the 60 consecutive nights of observation, i.e. in this particular case (HR1099) over a total of 21 stellar rotations. Comparable data were obtained recently as support for the Gravity probe B mission for IM Peg (K2III, RS CVn binary; Marsden et al. 2007).

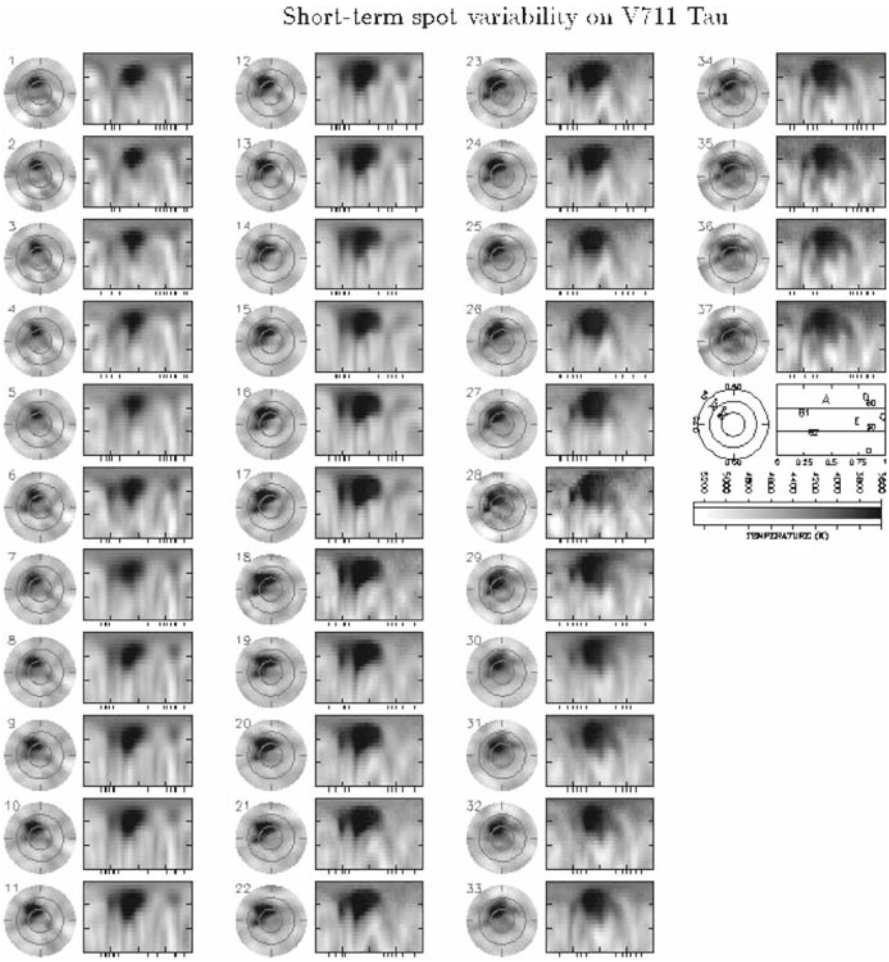

Fig. 6 Short-term evolution of starspot on the RS CVn subgiant V711 Tau = HR1099. Shown are 37 consecutive Doppler images in pole-on projection (*left columns*) and in Mercator projection (*right columns*). The total time series spans 57 nights. The *grey scale* represents temperature as indicated in the *last subpanel*. The *empty panel* indicates the surface latitudes and longitudes along with the positions of the main spot features. The *thick marks* beneath each Mercator plot represent the times of observation. Data obtained at the NSO McMath–Pierce telescope (Strassmeier and Bartus 2000)

Such data, if based on longer time sequences and analysed more quantitatively, could be compared directly to white-light sunspot data. Attempts to detect and monitor such isolated spots are currently underway for a number of spotted stars in the STELLA project[10] (Strassmeier et al. 2004; Weber et al. 2009).

Given the short lifetime of sunspots of a month at most and a similar time scale for low-to-mid latitude starspots, it was a surprise to find the big polar starspots to be comparably long lived. Polar cap-like starspots appear to have lifetimes of over a

[10] http://www.aip.de/stella.

decade, in RS CVn binaries as well as in young main-sequence stars. Holzwarth et al. (2006) concluded that polar spots are likely due to the influence of strong meridional circulation (polewards on the surface) and that the intermingling of polarities in the polar regions favours the higher flow velocities needed for that scenario. Obviously, polar spots may have a different formation history than low-to-mid latitude spots and their lifetimes may not be directly comparable.

Işik et al. (2007a,b) computed the flux evolution and the lifetimes of bipolar and unipolar starspots based on a magnetic flux transport model and found that varying the surface flows and the tilt angles modified the spot lifetime over a range of 1 month. Comparable decay patterns and lifetimes were found for monolithic starspots and for conglomerates of smaller spots of similar total area that could add a lifetime of up to 7 years for big polar caps. Işik et al. (2007a,b) coupled model of magnetic flux generation and transport verifies the increasing pole-ward deflection of emerging flux tubes with high angular velocities but also supports the polar magnetic-region accumulation picture put forward by Schrijver and Title (2001). While the toroidal field contour at the bottom of the convection zone almost exactly coincides with the surface emergence pattern for a slow rotator as the Sun, it markedly differs for fast rotators. Figure 7 from Işik et al. (2007a,b) shows that the tilt angles of the toroidal field contour (with respect to the equator) become much larger with shorter rotation period. For the case $P = 2$ days, a tilt angle of 35° leads to two latitudinal bands of dominant flux emergence with opposite polarity. Meridional transport of this flux leads to strong polar fields with field strengths of up to 30 G. Whether these could be related to the recent discovery of high-latitude kG fields on the Sun (Tsuneta et al. 2008) remains to be determined.

14 Spot-related velocity fields

Granules and supergranules are the best known tracers of local photospheric velocity fields on the Sun. The otherwise symmetric granular pattern is disrupted at the rim of a sunspot and replaced by the penumbral inflow and outflow (the "Evershed" effect). Because sunspot umbrae are not completely dark—and the residual intensity measured is too high to be alone from radiative energy transport—some convective energy transport likely occurs and a granular pattern indeed has been observed in the 2,000-K cooler spot umbrae (Tritschler and Schmidt 2002). However, the actual complexity of flows around sunspots has been revealed by SOHO/MDI helioseismic data. Zhao et al. (2001) reconstructed mass flow fields across a sunspot at depths between 0 and 12 Mm. They found rings around sunspots of downflow at a depth of 0–3 Mm and upflow at a depth of 5–8 Mm with almost no flow directly below the umbra. Some rapidly spinning spots show horizontal flows into the umbral region at depth between 0 and 3 Mm but out of the umbral region at depths between 9 and 12 Mm (Kosovichev 2002). Bright rings around Sunspots were observed earlier already in the late seventies and are explained as the result of heat transport by the underlying flow and the increased thermal diffusivity due to reduced magnetic quenching around spots (Kitchatinov and Rüdiger 2007). Also, magnetic flux tubes appear to represent a tree-like structure in the upper convection zone that supports Parker (1979) original cluster model, but see

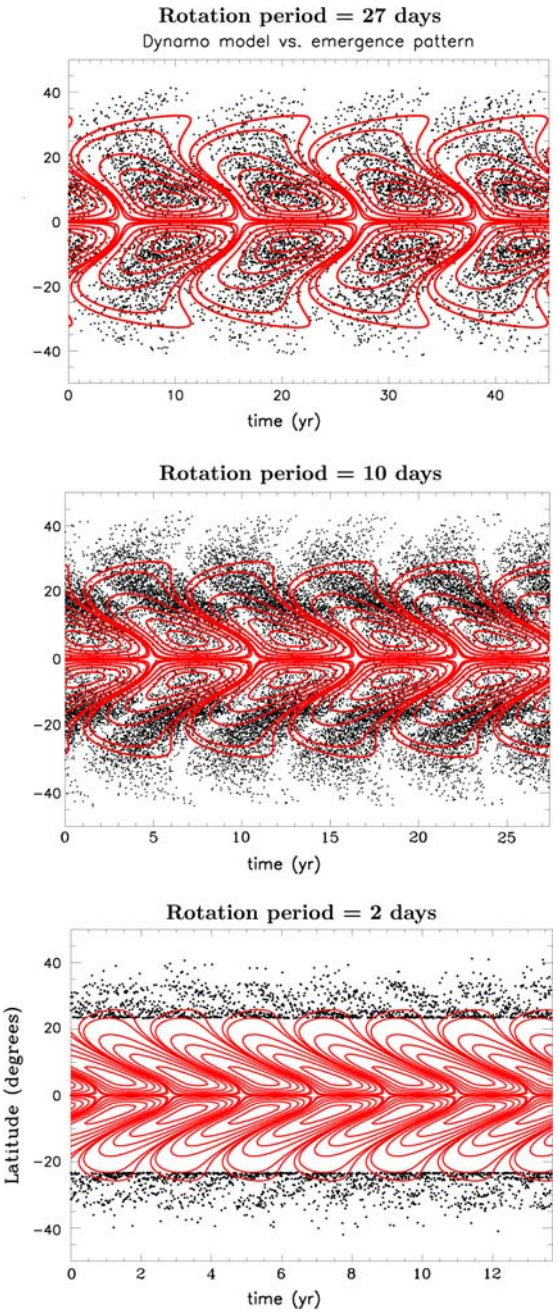

Fig. 7 Time-latitude diagrams of a dynamo-generated mean toroidal magnetic field at the bottom of the convection zone (*contours*). The *dots* are the emergence points of flux loops. Shown are simulations of a solar-like star with three different rotation periods of 27, 10, and 2 days (from *top* to *bottom*). Note that for the very fast rotator, $P = 2$ days, the emergence pattern is shifted significantly towards the rotational poles and does not agree with the dynamo wave anymore (Işik et al. 2007a,b)

Rempel et al. (2008) for a comparison with their new three-dimensional MHD sunspot model.

Of course, for starspots such detail is not available. However, line-bisector variations in phase with the rotation period were found, e.g. on the G8 dwarf ξ BooA

(Toner and Gray 1988). This has been attributed to a surface feature carried across the stellar disk by stellar rotation with a vertical velocity field enhanced over that of the rest of the surface. Toner and LaBonte (1990) also investigated the possibility that these line bisector variations may be caused by a mass flow tangential to the surface ("moat flow"). The latter model produces an equally good fit to the observations. A first pseudo 3-D Doppler image of the very active K subgiant in the HU Virginis RS CVn binary showed strong chromospheric outflow associated with a large photospheric spot on one hemisphere but inflow associated with a second, small, but warm spot located almost 180° apart (Strassmeier 1994). Follow up of this star revealed a huge X-ray flare (Endl et al. 1997) suggesting a connective loop of length one stellar radius, with mass exchange between these two spots (or spot regions). A similar phenomenon was likely seen in the Doppler images of XX Tri where the huge single spot shown in Fig. 5 had a warm (but much smaller) equatorial counterpart on the backside of the star. The large (averaged) temperature difference of the two hemispheres then caused the record V-band amplitude of 0.63 mag. These features were generally on opposite hemispheres 180° apart in longitude and we speculate that they might be related to the flip–flop phenomenon mentioned earlier.

Spinning sunspots (discovered 100 years ago by Evershed 1910) do not yet have a stellar counterpart discovered. Recent solar observations with the white-light channel on TRACE have shown sunspots to rotate by up to 200° about their umbral centre within 3–5 days (Brown et al. 2003). Its cause is either in the photospheric flow pattern made up by the different shear due to differential rotation and by local proper motions due to magneto-convective dynamics, or it is caused by the direct emergence of a twisted flux tube that causes its (photospheric) footpoints to rotate around each other. The observations of Brown et al. (2003) excluded the effects of surface differential rotation as the cause of the rotation due to a number of reasons (rotation direction must be opposite in the adjacent hemispheres, larger spots must be rotating faster than smaller) but could not conclude on a single mechanism. The twisted flux-tube picture requires the opposite polarity of the observed sunspot to anti rotate, which is mostly not observed. Clearly, if starspots were to experience the same mechanism, likely it could constrain only macroscopic effects like the overall photospheric flow pattern around starspots. Among the immediate goals for stellar astronomers should be the identification of the polarities of starspots. Indeed, using VLT/FORS-1 measurements of the longitudinal magnetic field of FK Com in conjunction with Doppler imaging, Korhonen et al. (2009) presented first evidence that the two large active regions on FK Com had opposite polarities.

From solar analogy, we may assume that the presence of a large starspot would also disturb a large-scale, possibly even global, photospheric velocity pattern because the magnetic field will likely penetrate a much larger volume around it than what would be seen as a spot. First attempts to measure large-scale surface flows on a star other than the Sun were presented by Kővári et al. (2007a,b), Vida et al. (2007) and, Švanda et al. (2009, in preparation). E.g., Švanda et al. applied the method of local correlation tracking (Švanda et al. 2006) to 28 Doppler images of LQ Hya and obtained an average stellar surface flow map over a period of two months (shown in Fig. 8). An average poleward meridional flow of 80 m/s and a convergent flow around spots in the range of up to several hundred m/s was possibly detected. This is to be compared to

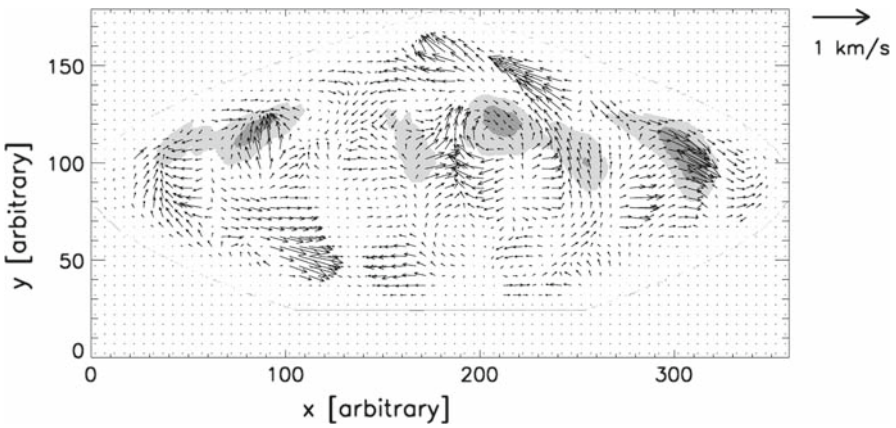

Fig. 8 Flows (*arrows*) in the photosphere of the rapidly rotating K-dwarf LQ∼Hya. The projection style is true-area Aitoff. The length of the arrows is scaled by the actual radius of the stellar disc in solar units (1 km/s is shown to scale in the *top right corner*). The background *grey-scale* image is the first map used in the series of 28 Doppler maps to recover the flow field. There appear to be two distinct flow structures; a general poleward flow and a network of convergent flows around spots. Based upon preliminary results by Švanda et al. (2009, in preparation)

the maximum 15 m/s observed at mid-heliographic latitudes on the Sun. The amount and the sign of the differential rotation appear in agreement with previous studies. Furthermore, they possibly found evidence for the existence of convergent flows towards the centre of starspots, which appears to be consistent with sunspot measurements obtained from local helioseismology. However, the findings are not conclusive yet and more and better data are desperately needed.

An extreme star in terms of its long rotational period of 307 days is the single, active G8 giant HR1362 (EK Eri). Such border cases may be important for a better understanding of starspots. Recently, Dall et al. (2009, in preparation) obtained ultra-precise radial velocities with ESO's HARPS spectrograph and detected a 100 m/s radial velocity amplitude in phase with the 307-day period light curve. Line bi-sector shapes as well as the normalized CaII H&K emission line fluxes varied in phase with the optical light curve. This suggests a strong correlation between the cool spots that modulate the light curve and the velocity fields that modulate the bisectors. Additionally, a short ≈1 h velocity modulation with an amplitude of 0.5 m/s was detected during three nights of dedicated monitoring (the noise in this HARPS time series was just 40 cm/s). Dall et al. (2009) interpreted this as solar-like oscillations. If real, this would be the first such detection on an active spotted giant star. Also recently, and fully independently, Auriere et al. (2008) succeeded in measuring a mean surface magnetic field of 270 G for EK Eri, with a geometry predominantly poloidal. Such a field would be direct evidence for a dipolar structure unusual for an active, cool star and thereby suggestive of the star's proposed Ap-star history, as put forward by Stępień (1993) and Strassmeier et al. (1999a,b). After all, we may conclude that even the dynamo-dominated cool stars preserve their original seed field, and also that, if the dynamo efficiency is just low enough, its signature becomes observable on the surface.

15 Magnetic fields from Zeeman–Doppler imaging

All available optical and infrared magnetic-field measurement techniques are based on the Zeeman effect—either in terms of splitting (e.g. Johns Krull et al. 2004) or of polarization (e.g. Donati and Brown 1997)—and the closely related Paschen–Back and quadratic Zeeman effects (e.g. Euchner et al. 2002). It allows the detection of magnetic fields ranging from μG in starless clouds and the interstellar medium (but see also Cox et al. 2007), via the kG-fields on the surfaces of the Sun and solar-like stars to some white dwarfs with fields well in excess of 1 MG (Wickramasinghe and Ferrario 2000; Jordan 2009). A 1-kG field produces a Zeeman splitting in the spectrum of a cool star that is approximately equal to the thermal width of a typical neutral atomic line, making it possible to map the geometry and strength of the magnetic field on the surface of point-like sources (Semel 1989). The transfer of radiation in a magnetized plasma is a key ingredient for the successful separation of the surface field components, i.e. azimuthal, toroidal and poloidal (Degl'Innocenti and Landolfi 2004; Piskunov and Kochukhov 2002; Carroll et al. 2008; Trujillo-Bueno 2009). Except for unresolved mixed-polarity magnetic fields, the many mechanisms for scattering and depolarization are negligible for the detection of Zeeman polarization from fields stronger than approximately 100 G (for details see Stenflo 2002, "*polarized radiation diagnostics of stellar magnetic fields*"). However, no magnetized model atmospheres are available so far, neither theoretical nor semi-empirical ones, and the subtle effects of Faraday rotation in a cool-star atmosphere remain neglected despite that magnetic flux structures in equipartition have a decisive impact on the temperature structure, as those on the Sun (e.g. Carroll and Staude 2001). First attempts to incorporate magnetic effects into the computation of (magnetic Cp-star) model atmospheres were presented recently (Shulyak et al. 2009).

We do not know much about the magnetic field of a starspot itself, despite that the Zeeman–Doppler imaging (ZDI) technique successfully disentangles the polarity distribution across the stellar surface (see Fig. 3 for the principle). A common interpretation problem of ZDI maps is that one detects preferably the polarization signature of surface structure that appears bright rather than faint as starspots. Many reconstructions of the rapidly rotating single K-dwarfs AB Dor and LQ Hya or the K sub-giant component of HR1099 showed such a non-correlation (e.g. Donati et al. 2003). Figure 9 shows the K subgiant II Pegasi as another recent example. One reason is likely that starspots not only consist of a radial field alone but also have other field components of comparable strength, i.e. an azimuthal and a toroidal field, possibly in a geometry comparable to a sunspot penumbra. If so, the full Stokes vector is needed to uniquely disentangle the field across the surface (Kochukhov and Piskunov 2006). More obvious, however, is the crosstalk between radial versus meridional fields for the reconstruction of spots at lower latitudes. The surface-integrated Stokes-V signature for spots with an azimuthal field is basically antisymmetric with respect to the meridian passage while for spots with radial or meridional fields it is symmetric (Donati and Brown 1997; Rice 2002). Carroll et al. (2007) found that their surface field reconstructions for II Peg in Fig. 9 exhibited a strong imbalance in the magnetic polarity and suggested that this imbalance results to a large extent from the inability of the circular polarization signal to capture the whole magnetic flux of the star. It

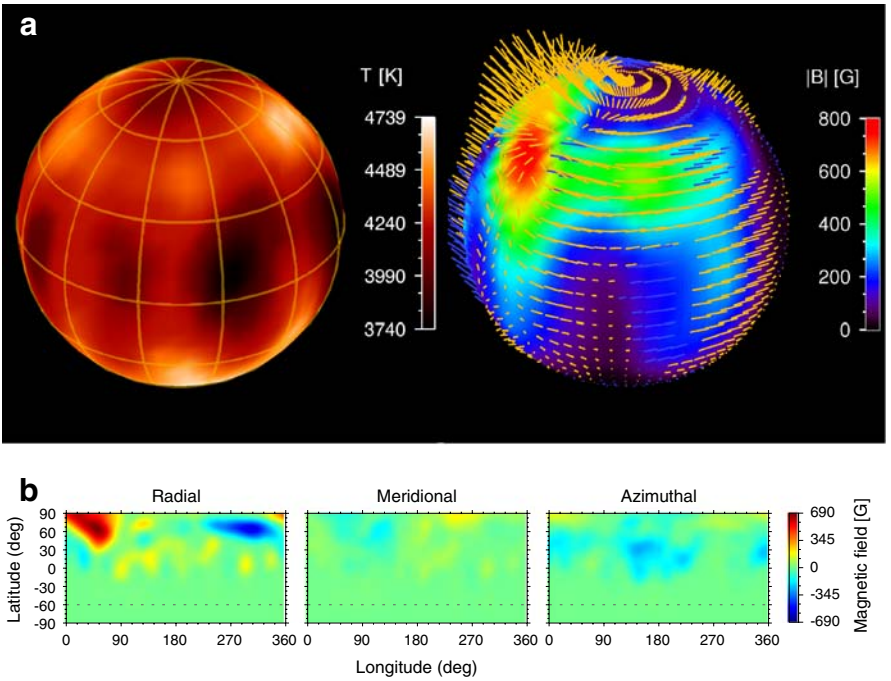

Fig. 9 **a** Temperature map (*top left*) and surface magnetic field map (*top right*) of II Pegasi from 2007. Both maps are reconstructed simultaneously from atomic lines. The "needles" in the *right* image indicate the field vector for each surface pixel, the *colour* represents the absolute field strength. Note that the regions with cool spots have almost no magnetic field detections. **b** The same map but split into its radial, meridional, and azimuthal field components in pseudo Mercator projection. Images based on Carroll et al. (2007)

appears that circular polarization alone, i.e. Stokes V, does not, first, allow to identify the field signatures from within the cool spots and thus establish a sunspot analogy or contradict it and, second, allow the unique reconstruction of all field components at all latitudes. With this inherent uncertainty in mind it is particularly challenging to use current photospheric ZDI maps as a boundary condition to extrapolate the overlaying coronal field via force-free field extrapolations.

Another approach to disentangle starspot magnetic fields was already proposed back in the 1980s by Vogt (1979), Ramsey and Nations (1980) and Vogt (1981b). They suggested to search for the increased molecular contribution in high-resolution optical and infrared spectra due to cool starspots. However, the first synthetic molecular Stokes spectra were presented only recently by Berdyugina et al. (2000a,b). Afram et al. (2007) have analysed the usefulness of FeH, MgH and TiO spectra as diagnostic tools for studying starspots with the molecular Zeeman and Paschen–Back effects. They presented molecular line profiles obtained by assuming magnetic fields of 2–3 kG and compared these synthetic Stokes profiles with spectro-polarimetric observations in sunspots. Good agreement was found and now provides a tool to study the coolest parts of starspots. First direct detections based on Stokes V profiles of the TiO7055 band were recently reported for five active stars (V833 Tau, AU Mic, FK Aqr, EV Lac,

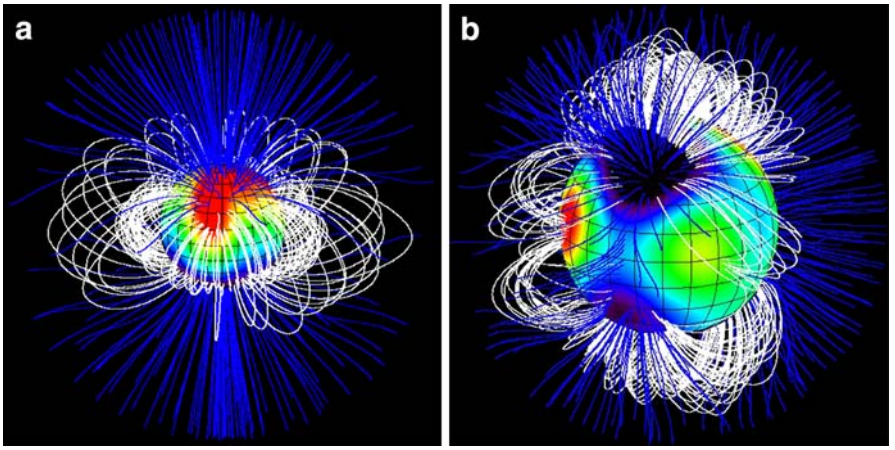

Fig. 10 The coronal field of **a** V374 Peg (M4V) and **b** τ Sco (B0V). The magnetic field lines are potential-field extrapolations based on the observed photospheric field distribution. Quite surprisingly, the field distribution on the massive B0 star compares to that of the solar corona while the low-mass star's field more resembles a purely dipolar structure. Images courtesy of J.-F. Donati and M. Jardine, see text

V1054 Oph) by Berdyugina et al. (2008). The stronger detections of these were for the four M stars in the sample and indicate a single-polarity magnetic field covering at least 10% of the stellar disk. A Stokes V signal in the TiO bands was also detected for the two late-type K stars (V833Tau and II Peg) but with very low amplitudes in the 0.1–0.2% range. Along with the possible polarity separation for spots on FK Com by Korhonen et al. (2009), this result appears to be the first detection of the magnetic field of starspots.

16 Starspots and coronal fields: a direct connection

Multi-polar solar active regions are the hosts of the rather inhomogeneous solar coronal magnetic structure with its many loops and associated energetic events visible in the extreme ultraviolet and at X-ray wavelengths. The TRACE movies have shown us their complexity and how quickly such loops evolve (e.g. Aschwanden et al. 2000). Abundant evidence is available in the literature that such loops also exist on other stars of spectral type F to K, in particular from stellar X-ray data (e.g. Güdel 2007). However, is there also evidence from spatially resolved stellar-disk observations?

Figure 10 not only gives the answer but also compares two extreme stellar cases: the M4 dwarf V374 Pegasi (Donati et al. 2006a; Morin et al. 2008) and the B0 dwarf τ Sco (Donati et al. 2006b). While the M4 star is old and has a mass of just 0.28 M_{Sun} and a rotation period of 0.44 days, the B0 star is very young and has a mass of 15 M_{Sun} but rotates comparably slowly with a rotation period of 41 days. It is also among the strongest stellar X-ray sources. Both stars' coronal fields were derived by a numerical extrapolation of a force-free field from the observed photospheric magnetic field as obtained from a Stokes-V Zeeman Doppler image. Surprisingly, the M4 star shows a comparably simple global field structure rather than the expected chaotic geometry

predicted from a non-axisymmetric dynamo (see later in Fig. 14). The B0 star, on the other hand, surprised with an arch-like network of surface fields, most likely the relic from the star's formation age rather than a dynamo-induced field (Donati et al. 2006b). The latter argument is mainly based on the observation that the toroidal field component relative to the poloidal one is much weaker than what is usually seen for stars with convective envelopes. It is also supported by the fact that the field of τ Sco appeared stable over the 1.5-year period of observations. It appears that the arch structure accelerates the energetic particles towards the loop summits where they shock and then cause the emission of large amounts of X-rays, as observed. Therefore, the τ Sco loop structure more resembles solar analogy than the structure on the M4 star.

More surprises are likely ahead, in particular when we apply the DI and ZDI techniques to more "exotic" stars. One class of stars that keeps focusing our attention are the young, low- mass weak-line T Tauri stars (wTTS; e.g. Montmerle 2003). These stars still carry the star- and planet-formation signatures but can be compared to young main-sequence stars, and thus are thought to link these two important phases of stellar evolution. Two examples are V4046 Sgr (Stempels and Gahm 2004), a close binary pair with a circum-binary disk, and MN Lup (Strassmeier et al. 2005), a single rapidly rotating wTTS also with an accretion disk. Photospheric absorption line profiles are not easily found in this class of stars but the neutral lithium line at 670.8 nm is sometimes an exception. Its line profile variations (Fig. 11a) can be used to infer the surface spot distribution. And indeed, Doppler imaging of the surface of MN Lup revealed several high-contrast spots at high latitudes (Fig. 11b). However, these spots are due to accretion post-shock heating in the photosphere rather than due to cool photospheric spots or warm chromospheric plages as for active cool stars, which is unexpected for a weak-lined, or sometimes called "naked", T Tauri star. The spots' locations are still determined by a magnetic field though but, in the case of MN Lup, by a global dipolar field reconnected with the accretion disk. We may only speculate how the field geometry would look for a close pair of such stars, as in the case of V4046 Sgr. Both V4046 Sgr components, together with their co-rotating coronal clouds, are located well inside the edge of the circum-binary disk, and also inside the co-linear Lagrangian points of this binary (Montmerle 2009, private communication).

17 Starspots and transiting exoplanets

A particularly "beautiful" light curve of a spotted star was delivered by the CoRoT satellite in its second announced planet discovery dubbed CoRoT-Exo-2*b*. The planet host star—the *a* component—is a spotted G7 main-sequence star. It shows a classical double migrating wave due to two starspots or starspot groups with different rotational periods. While Alonso et al. (2008) used the folded light curve from 78 planetary transits with an orbital period of 1.743 days to obtain the planet's parameters (Radius $= 1.5\mathrm{R}_{\mathrm{Jupiter}}$, Mass $= 3.3\mathrm{M}_{\mathrm{Jupiter}}$), Lanza et al. (2009) performed time-series spot modelling of the stellar light curve to obtain the star's longitudinal spot distribution. The amplitude and the scatter in the out-of-transit light curve reached a level of up to ≈ 70 and ≈ 0.1 mmag, respectively. The 2.5-min binned phase-folded light curve was even affected by successive occultation of stellar active regions by the

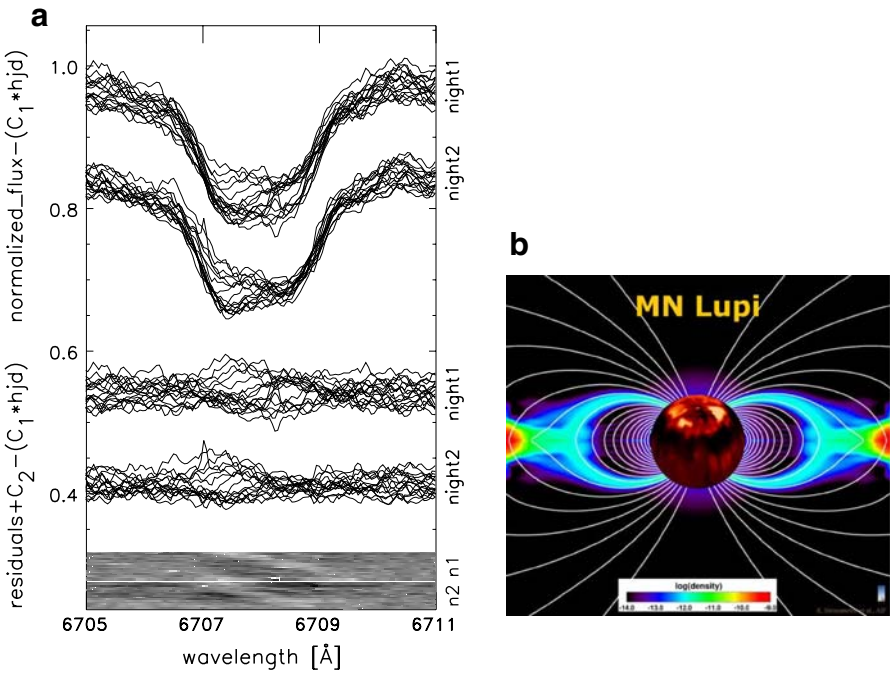

Fig. 11 **a** Photospheric line profiles of the wTTS MN Lupi. Shown are two time series from two stellar rotations ($P = 0.44$ days) on two consecutive nights as indicated. The offset between the two nights is just for presentation purpose. The *bottom* part of the figure shows the residuals from the average profile as lines (*middle*) and as grey-scale plots (*bottom*). Note the changes of the profile shape due to the migration of cool spots across the stellar disk. **b** Observed temperature Doppler map of MN Lup (central map). *Black* is −500 K; white is +2,000 K with respect to the effective temperature of 3,400 K. The background shows the numerically simulated magnetic field and the (logarithmic) density of the disk. The high-latitude hot spots on the surface of MN Lup are not classical starspots, but are the impact locations from accretion-disk material funnelled onto the star along reconnected polar magnetic field lines. Their impact latitudes on the stellar surface constrain the simulated poloidal field strength to 3 kG, based on the magneto-static funnelling model of Küker et al. (2003). Doppler image from Strassmeier et al. (2005)

planet. A detailed spot-model fit to the data (Fig. 12, left panel) revealed two active longitudes approximately 180° apart, with the spots of one longitude suggesting a period of 4.5221 days and the spots of the other longitude a period of 4.5543 days. If interpreted as differential rotation, this indicates a significantly weaker differential rotation than on the Sun, about 1 per cent. From contemporaneous ground-based data, Bouchy et al. (2008) report on a spectroscopic transit observed with the high-precision spectrographs SOPHIE and HARPS.

Pont et al. (2007) monitored three transits of the giant gas planet around the nearby K dwarf HD 189733 with the ACS camera on the HST. These data revealed clear evidence of the planet occulting two spots on the surface of this star. At least one large spot complex of $>80,000$ km in longitude and $\approx 12,000$ km in latitude (a large sunspot group) with a ΔT of >100 K is required to explain the observed flux residuals and their colour evolution. The spot occultations were recorded during three HST visits and indicate a latitude higher than expected from solar spot analogy. Note that these

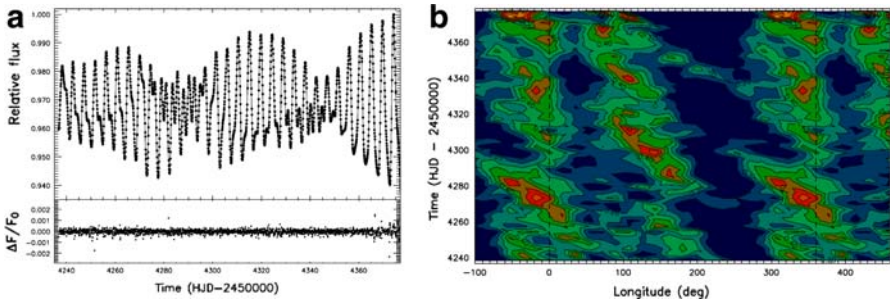

Fig. 12 The COROT light curve of CoRoT-Exo-2 with the planetary eclipses removed. **a** The host star's light variability with a period of 4.522 days is due to starspots. The light curve changes from single humped to double humped and back, and is the classic sign of two spots at different latitudes on a differentially rotating stellar surface. Its full amplitude at the end of the series is 7% in the CoRoT integral-light bandpass (the star's V brightness is 12.57 mag) proportional to ≈20% surface spottedness. The line is a fit with a time-dependent spot model shown in the *right panel* **b** (the *subpanel* shows the normalized residuals from the fit). **b** Spot-longitude distributions as a function of time. Time runs vertical from bottom up. Note the two active longitudes (see text, Lanza et al. 2009)

data likely reached a record signal-to-noise for time-series (night-time) astrophysics: 35,000:1 for a 10-min interval or 15,000:1 for an individual measurement.

Furthermore, if the same spot is eclipsed on at least two consecutive transits, it is also possible to measure the stellar rotational period at the spot's latitude (schematic in Fig. 13a). Brown et al. (2001) detected two starspots on more than one transit of HD 209458, observed again by the HST in 2000 (Fig. 13b). Using these data, Silva-Valio (2008) found a stellar rotation period of either 9.9 or 11.4 days, depending on which spot is responsible for the signature in the light curve a few transits later. Comparison with period estimates of HD 209458 reported in the literature indicates that 11.4 days is the most likely stellar rotation period.

Starspots are intrinsic noise for planet hunters. Several groups have shown that the influence of a spotted stellar disk for precise radial-velocity measurements can be of much higher significance than the planet-induced signal itself (see, e.g. Hatzes 2002). A radial-velocity amplitude of up to ≈100 m/s for even slowly rotating stars with a very modest spot coverage is expected. Saar and Donahue (1997) and Hatzes (2002) gave a relationship of velocity amplitude A in m/s with spot coverage f in per cent and line broadening $v \sin i$ in km/s ($A = (8.6 v \sin i - 1.6) f^{0.9}$). This is well seen in the data of CoRoT-Exo-2b by Bouchy et al. (2008). A similar linear relationship is expected for the velocity span of line-bisector variations due to starspots which was observationally confirmed for the spotted star HD 166435 by Queloz et al. (2001). A comparable conclusion was reached recently for the wTTS LkCa19 by Huerta et al. (2008).

Beckers (2007) voiced some concerns with regard to a unique interpretability of long-term radial velocities at the 1 m/s level. This concern is particularly worrisome for the search for Earth-like masses in habitable zones where one has to worry about more subtle effects from the integrated light of the host star than just its starspots. Based on solar Doppler observations, Beckers (2007) disk integrated the effects of global meridional motion as a function of the 11-year cycle and found a radial-veloc-

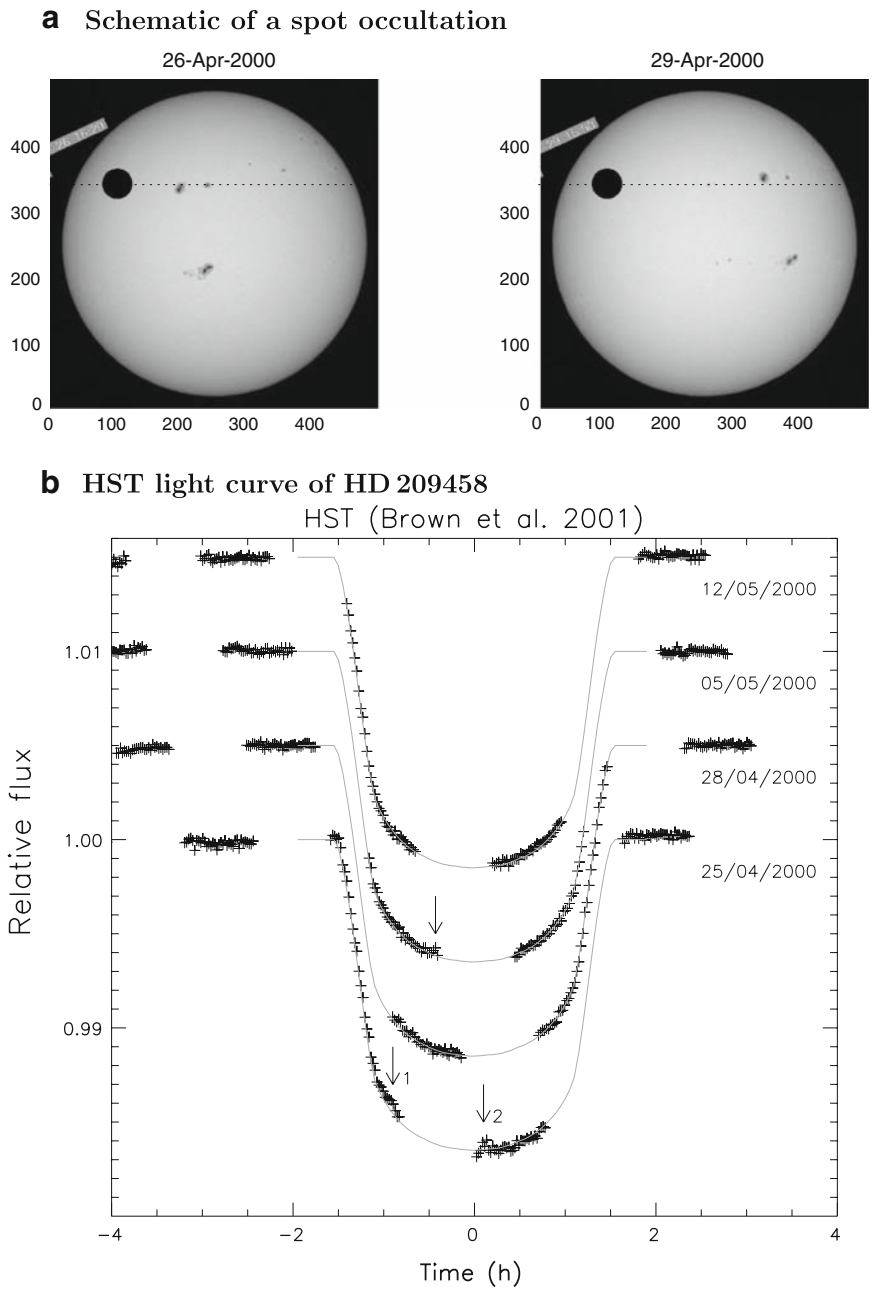

Fig. 13 **a** Schematic presentation of an exoplanet transit with a real image of the Sun in the background. The exoplanet transit path is indicated as a dashed line for two visits with the HST on April 26 and 29, 2000. **b** Four transit light-curves (*plusses*) of HD 209458 showing the light-curve deformations due to the eclipse of two spots (marked with an *arrow* as "1" and "2") (Silva-Valio 2008)

ity amplitude (peak-to-valley) of up to 5 m/s for $i = 0°$ (pole-on view) to 1.6 m/s for $i = 60°$ (the amplitude at $i = 90°$ becomes larger again due to the more complex latitude dependency of solar meridional flow). As a comparison, note that Earth causes an annual 0.2 m/s full amplitude on the solar radial velocity, an effect ten times smaller.

18 Starspots and stellar evolution

A remaining but central scientific question is whether dynamo-generated magnetic fields impact stellar evolution or not. Stellar evolutionary MHD models are not available yet in order to make testable predictions for observers, in particular not for low-mass stars, but see Li et al. (2006) for first attempts. Observational (Landstreet et al. 2008; Hubrig et al. 2007) and theoretical (Maeder and Meynet 2004; Maeder et al. 2009) efforts are currently more mature for massive (in the proper respects simpler) stars with 10–15 solar masses. Interesting surprises are almost assured once state-of-the-art magneto-hydrodynamic codes become more standard. For example, Ziegler (2005) 3-D simulations of the core collapse of a one solar-mass pre-solar cloud ended up in a binary star once an overcritical vertical magnetic field was included!

However, any future attempts to code the impact of a magnetic field would greatly benefit from some a priori knowledge of the time scales involved. This is where starspot-related observations may help. A simple and—in principle—observable timescale for dynamo-generated magnetic flux can be extracted from the gradient of rotational evolution of low-mass stars in open clusters of well-defined age. One major uncertainty in explaining stellar rotation has to do with the timescale of internal angular momentum transport. At one extreme, one can have a very short timescale, implying solid-body rotation while a longer timescale would suggest increasing amounts of internal differential rotation (e.g. Barnes et al. 2001; Barnes 2007). The currently published (surface) rotation periods (e.g. Irwin et al. 2007) do not contain a sufficient number of intermediate-age stars to discriminate between the solid-body and differentially rotating models. More observations of rotation periods based on starspots are clearly needed and an attempt to do so is underway with robotic telescopes[11] and as part of the WIYN Open Cluster Study (e.g. Meibom et al. 2008) as well as from deep exoplanet transit searches (e.g. Hartman et al. 2008).

19 A unified solar and stellar dynamo spot theory?

The first MHD sunspot model was presented recently by Rempel et al. (2009). Their 3-D simulations showed penumbral structures with Evershed outflows along dark-laned filaments with nearly horizontal magnetic field which are embedded in a background of stronger and less inclined field, just as observed. The penumbral filaments result from magneto-convection in the form of hot rising plumes, which resemble the observed umbral dots. The latter were often interpreted as bundles of flux tubes, following the picture put forward by Parker (1979), a picture which we now possibly

[11] "The STELLA Open Cluster Survey".

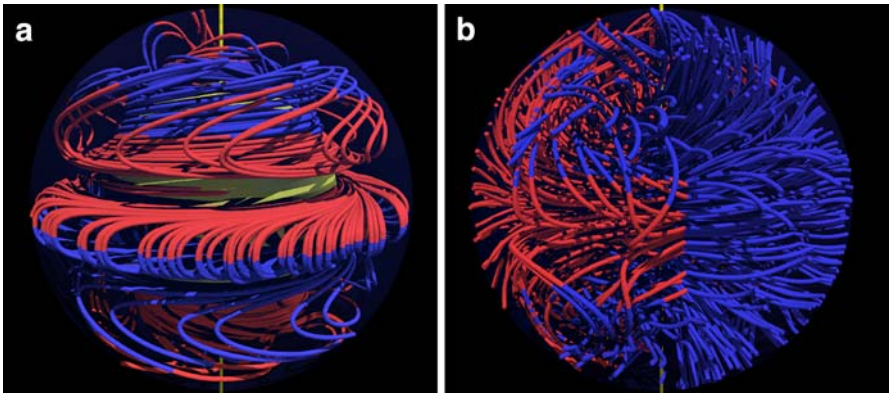

Fig. 14 Different dynamo processes lead to vastly different field geometries. The images show numerical simulations of the magnetic field in a stellar interior just below the surface. Red (or *brighter*) means the field is pointing outwards, blue (or *darker*) means the field points inwards. The *left* image, panel **a**, is for a solar-like star with a simple dipole (polarity in the southern hemisphere mirrors the polarity in the northern hemisphere). The *bottom* of the convection zone is indicated but is barely visible at mid latitudes. The *right* image, panel **b**, shows a non-axisymmetric dynamo in a fully convective star. There, polarity in the western hemisphere mirrors the polarity in the eastern hemisphere. Its field geometry is more chaotic. Figure and computations courtesy of R. Arlt, AIP

need to revise. It was already shown by Brandenburg (2005) that a global turbulent dynamo can produce a large-scale field, which could be compressed after some time to "local" dimensions by near-surface shear. Sunspot MHD simulations—in particularly when combined with local helioseismology—have the potential to bridge the gap from sunspots to starspots. Clearly, global MHD models should be invoked to explain the over-dimensioned sizes and long lifetimes of starspots, rather than a scaling of the classical Parker model.

So far we have many pieces for a global dynamo theory, but no coherent picture, not even for the Sun. However, cornerstones for a successful (numerical) theory are likely the interface layers inside and outside the star. These interfaces are the tachocline at the bottom of the convection zone that acts as the interface to the stellar core, and the stellar surface that acts as the interface to the exterior. The tachocline likely dominates the dynamo itself, at least in a solar-like star, while the surface interface layer links the atmosphere and back-reacts on the outer layers of the convective envelope. The in-between, the convective layer, is the big playground for turbulent dynamo models. While it is known that turbulence can lead to a large-scale magnetic field, the time-scales of its growth may be very long. The results of detailed studies of how turbulence generates coherent fields over the size of the star will have implications for turbulence theory in general. The observation of starspots, in particular their decay, could lead to a better estimate of the magnetic diffusivity in the convective layer beneath the stellar surface and significantly contribute to the reliability of (solar) cycle predictions.

Figure 14 shows the results of two numerical simulations of a mean-field dynamo (Arlt, private commumication) illustrating a dynamo which is dominated by differential rotation and one dominated by convection. Full MHD simulations of fully convective stars were studied by Brandenburg (2002) and Brandenburg and Dobler (2002).

The results are among the extremes that we expect to encounter for cool stars. The wound-up field distribution in the simulation in the left panel of Fig. 14 arises for a tachocline interface appropriate for a solar-like G star, while the more chaotic field line distribution in the right panel of Fig. 14 is for an M star without a tachocline.

But not only spatial interfaces could dictate a dynamo's faith. Interior reconnection may also play a decisive role, at least during some later evolutionary stages, i.e. when the remnant of the original seed field that had gotten the dynamo running in the first place reconnects with the weakening dynamo field. However, whether such a frozen-in, remnant field still exists in later evolutionary stages or not is currently speculative at best. Are the interior fields of evolved, active G–K stars with their huge polar starspots possibly a mix of such different types of dynamos? What systematic indicators of dynamo-related magnetic fields versus frozen-in magnetic fields are there in the H–R diagram in the first place? Can we learn something from surface magnetic-field decay laws of spots on stars of vastly different ages? As usual, we must conclude that more systematic and, most important, more quantitative observations of stars with spots are needed. Therefore, I boldly suggest high-resolution spectro-polarimetric capabilities for the new generation of Extremely Large Telescopes, in particular for the European 42 m E-ELT or the US Thirty Meter Telescope and its proposed optical and NIR spectrographs. Only these giant scopes may cope with the faint Stokes signals of cool magnetic starspots and their impacts on stellar structure and evolution as well as its feedback to solar physics.

Acknowledgments Thanks are due to many colleagues working in the field and who made this topic a continuously flourishing one. In particular I would like to thank my mentors Douglas "Doug" Hall and William "Bill" Wehlau who got me going on this topic a number of years ago. Most recently, I have benefited a lot from many discussions with John Rice and Thorsten Carroll on issues of Doppler imaging and also with Katalin Oláh and Thomas Granzer on issues of light curve interpretations. On MHD and dynamo issues, Rainer Arlt shed some light into the far corners in the back of my brain. Not unimportantly, several grants along the way had made all this more manageable, in particular from the Austrian Fond zur Förderung der wissenschaftlichen Forschung (FWF), the Deutsche Forschungsgemeinschaft (DFG), the German Bundesministerium für Bildung und Forschung (BMBF), and the Ministerium für Wissenschaft, Forschung und Kultur (MWFK) of the State of Brandenburg in Germany. Finally, without my family I would probably herd cattle in the mountains of upper Styria (nothing bad with that though).

References

Aarum V, Berdyugina SV, Ilyin IV (1999) Doppler imaging of UX Ari. In: Karttunen H, Piirola V (eds) Astrophysics with the NOT. Tuorla Observatory, University of Turku, Finland, p 222

Afram N, Berdyugina SV, Fluri DM, Semel M, Bianda M, Ramelli R (2007) First polarimetric observations and modeling of the FeH $F^4\Delta - X^4\Delta$ system. Astron Astrophys 473:L1

Albregtsen F, Maltby P (1978) New light on sunspot darkness and the solar cycle. Nature 274:41

Alonso R, Auvergne M, Baglin A et al (2008) Transiting exoplanets from the CoRoT space mission. II. CoRoT-Exo-2b: a transiting planet around an active G star. Astron Astrophys 482:L21

Aschwanden MJ, Tarbell TD, Nightingale RW et al (2000) Time variability of the "Quiet" sun observed with TRACE. II. Physical parameters, temperature evolution, and energetics of extreme-ultraviolet nanoflares. Astrophys J 535:1047

Auriere M, Konstantinova-Antova R, Petit P et al (2008) EK Eri: the tip of the iceberg of giants which have evolved from magnetic Ap stars. Astron Astrophys 491:499
Baliunas SL et al (1985) Time-series measurements of chromospheric CaII H and K emission in cool stars and the search for differential rotation. Astrophys J 294:310
Baliunas SL, Donahue RA, Soon WH et al (1995) Chromospheric variations in main-sequence stars. Astrophys J 438:269
Barnes JR, Collier Cameron A (2001) Starspot patterns on the M dwarfs HK Aqr and RE 1816 +541. MNRAS 326:950
Barnes JR, Collier Cameron A, Donati J-F et al (2000) Doppler images from dual-site observations of southern rapidly rotating stars—I. Differential rotation on PZ Tel. MNRAS 314:162
Barnes JR, Collier Cameron A, James DJ et al (2001a) Doppler images from dual-site observations of southern rapidly rotating stars—II. Starspot patterns and differential rotation on Speedy Mic. MNRAS 324:231
Barnes JR, Collier Cameron A, James DJ et al (2001b) Further images of α Persei G dwarfs. MNRAS 326:1057
Barnes JR, Collier Cameron A, Lister T, Pointer G, Still MD (2005) LO Peg in 1998: star-spot patterns and differential rotation. MNRAS 356:1501
Barnes JR (2005) The highly spotted photosphere of the young rapid rotator Speedy Mic. MNRAS 364:537
Barnes SA (2007) Ages for illustrative field stars using gyrochronology: viability, limitations, and errors. Astrophys J 669:1167
Barnes SA, Sofia S, Pinsonneault MH (2001) Disk locking and the presence of slow rotators among solar-type stars in young star clusters. Astrophys J 548:1071
Beckers J (2007) Can variable meridional flows lead to false exoplanet detections? Astronomische Nachrichten 328:1084
Berdyugina SV (2002) Sunspot and starspot interiors as seen from molecular lines. Astronomische Nachrichten 323:192
Berdyugina SV (2005) Starspots. Living Rev Solar Phys 2:8
Berdyugina SV (2007) Flip-flop cycles in solar and stellar activity. Highlights Astron 14:275
Berdyugina SV (2009) Observational evidence for magnetic fields across the H-R diagram. In: Strassmeier KG, Kosovichev A, Beckman J (eds) IAU symposium 259, cosmic magnetic fields: from planets, to stars and galaxies. Cambridge University Press, London, p 323
Berdyugina SV, Berdyugin AV, Ilyin I, Tuominen I (1998) The active RS Canum Venaticorum binary II Pegasi. II. Surface images for 1992–1996. Astron Astrophys 340:437
Berdyugina SV, Berdyugin AV, Ilyin I, Tuominen I (1999) The active RS Canum Venaticorum binary II Pegasi. IV. The spot activity cycle. Astron Astrophys 350:626
Berdyugina SV, Berdyugin AV, Ilyin I, Tuominen I (2000a) The long-period RS CVn binary IM Pegasi. II. First surface images. Astron Astrophys 360:272
Berdyugina SV, Frutiger C, Solanki S, Livingston W (2000b) Successful spectral synthesis of Zeeman-split molecular bands in sunspot spectra. Astron Astrophys 364:L101
Berdyugina SV, Berdyugin AV, Ilyin I, Tuominen I (2001a) IM Peg: first surface images. In: Garcia Lopez R et al (eds) 11th Cambridge workshop, cool stars, stellar systems, and the sun, ASP conference series 223, CD-ROM
Berdyugina SV, Ilyin I, Tuominen I (2001b) LQ Hya: surface images for 1993–1999. In: Garcia Lopez R et al (eds) 11th Cambridge workshop, cool stars, stellar systems, and the sun, ASP conference series 223, CD-ROM
Berdyugina SV, Usoskin I (2003) Active longitudes in sunspot activity: century scale persistence. Astron Astrophys 405:1121
Berdyugina SV, Fluri DM, Afram N, Suwald F (2008) First detection of magnetic fields in starspots and stellar chromospheres. In: van Belle GT (ed) 14th Cambridge workshop, cool stars, stellar systems, and the sun, ASPC 384, p 175
Biermann L (1938) Konvektion im Inneren der Sterne (II). Astronomische Nachrichten 264:361
Biermann L (1948) Konvektion in rotierenden Sternen. Z Astrophysik 25:135
Binnendijk L (1970) The orbital elements of W Ursae Majoris systems. Vistas Astron 12:217
Bouchy F, Queloz D, Deleuil M et al (2008) Transiting exoplanets from the CoRoT space mission. III. The spectroscopic transit of CoRoT-Exo-2b with SOPHIE and HARPS. Astron Astrophys 482:L25
Bouvier J, Bertout C (1989) Spots on T Tauri stars. Astron Astrophys 211:99
Brandenburg A (2002) Hydromagnetic turbulence in computer simulations. Comput Phys Commun 147:471

Brandenburg A (2005) The case for a distributed solar dynamo shaped by near-surface shear. Astrophys J 625:539
Brandenburg A, Dobler W (2002) Solar and stellar dynamos—latest developments. Astronomische Nachrichten 323:411
Brown DS, Nightingale RW, Alexander D et al (2003) Observations of rotating sunspots from TRACE. Sol Phys 216:79
Brown TM, Charbonneau D, Gilliland RL, Noyes RW, Burrows A (2001) Hubble space telescope time-series photometry of the transiting planet of HD 209458. Astrophys J 552:699
Buscher DF, Haniff CA, Baldwin JE, Warner JP (1990) Detection of a bright feature on the surface of Betelgeuse. MNRAS 245:7
Cameron R, Schüssler M (2007) Solar cycle prediction using precursors and flux transport models. Astrophys J 659:801
Carroll TA, Kopf M, Ilyin I, Strassmeier KG (2007) Zeeman-Doppler imaging of late-type stars: the surface magnetic field of II Peg. Astronomische Nachrichten 328:1043
Carroll TA, Kopf M, Strassmeier KG (2008) A fast method for Stokes profile synthesis. Radiative transfer modeling for ZDI and Stokes profile inversion. Astron Astrophys 488:781
Carroll TA, Staude J (2001) The inversion of Stokes profiles with artificial neural networks. Astron Astrophys 378:316
Catala C, Donati J-F, Shkolnik E, Bohlender D, Alecian E (2007) The magnetic field of the planet-hosting star τ Bootis. MNRAS 374:L42
Catalano S, Biazzo K, Frasca A, Marilli E, Messina S, Rodonó M (2002) Temperature and size of starspots from line depth ratios. Astronomische Nachrichten 323:260
Catalano S, Rodonó M (1967) Sulle variazioni della curva di luce del sistema RS CVn. Mem S A It 38:345
Chapman GA, Dobias JJ, Preminger DG, Walton SR (2003) On the decay rate of sunspots. GeoRL 30:27
Chou D-Y (1987) The cooling time scales of growing sunspots. Astrophys J 312:955
Chugainov PF (1966) New microvariable HD 117555. IBVS 172
Collier Cameron A (1992) Modelling stellar photospheric spots using spectroscopy. In: Byrne PB, Mullan DJ (eds) Surface inhomogeneities on late-type stars. Springer, Berlin, p 33
Collier Cameron A, Unruh YC (1994) Doppler images of AB Doradus in 1992 Jan. MNRAS 269:814
Collier Cameron A (1995) New limits on starspot lifetimes for AB Doradus. MNRAS 275:534
Collier Cameron A, Walter FM, Vilhu O et al (1999) Multisite observations of surface structures on AB Doradus in 1994 November. MNRAS 308:493
Cox NLJ, Boudin N, Foing BH et al (2007) Linear and circular polarization of diffuse interstellar bands. Astron Astrophys 465:899
Degl'Innocenti E, Landolfi M (2004) Polarization in spectral lines. Kluwer, Dordrecht
Dikpati M, Charbonneau P (1999) A Babcock-Leighton Flux transport dynamo with solar-like differential rotation. Astrophys J 518:508
Dikpati M, Gilman PA, de Toma G, Ghosh SS (2007) Simulating solar cycles in northern and southern hemispheres by assimilating magnetic data into a calibrated flux-transport dynamo. Sol Phys 245:1
Donati J-F (1999) Magnetic cycles of HR 1099 and LQ Hydrae. MNRAS 302:457
Donati J-F, Brown SF (1997) Zeeman-Doppler imaging of active stars. V. Sensitivity of maximum entropy magnetic maps to field orientation. Astron Astrophys 326:1135
Donati J-F, Collier Cameron A (1997) Differential rotation and magnetic polarity patterns on AB Doradus. MNRAS 291:1
Donati J-F, Brown SF, Semel M et al (1992) Photospheric imaging of the RS CVn system HR 1099. Astron Astrophys 265:682
Donati J-F, Collier Cameron A, Hussain GAJ, Semel M (1999) Magnetic topology and prominence patterns on AB Doradus. MNRAS 302:437
Donati J-F, Collier Cameron A, Semel M et al (2003) Dynamo processes and activity cycles of the active stars AB Doradus, LQ Hydrae and HR 1099. MNRAS 345:1145
Donati J-F, Forveille T, Cameron A et al (2006a) The large-scale axisymmetric magnetic topology of a very-low-mass fully convective star. Science 311:633
Donati J-F, Howarth ID, Jardine M et al (2006b) The surprising magnetic topology of τ Sco: fossil remnant or dynamo output? MNRAS 370:629
Donati J-F, Jardine M, Gregory SG et al (2007) Magnetic fields and accretion flows on the classical T Tauri star V2129 Oph. MNRAS 380:1297
Donati J-F, Jardine M, Gregory SG et al (2008a) Magnetospheric accretion on the T Tauri star BP Tauri. MNRAS 386:1234

Donati J-F, Mengel M, Carter BD (2000) Surface differential rotation and prominences of the Lupus post T Tauri star RX J1508.6-4423. MNRAS 316:699
Donati J-F, Moutou C, Fares R et al (2008b) Magnetic cycles of the planet-hosting star τ Bootis. MNRAS 385:1179
Donati J-F, Semel M, Carter B, Rees DE, Collier Cameron A (1997) Spectropolarimetric observations of active stars. MNRAS 291:658
Dunstone NJ, Hussain GAJ, Collier Cameron A et al (2008) The first magnetic maps of a pre-main-sequence binary star system—HD155555. MNRAS 387:481
Eker Z (1999) Reliability of light curves for photometric imaging. Astrophys J 512:386
Elstner D, Korhonen H (2005) Flip-flop phenomenon: observations and theory. Astronomische Nachrichten 326:278
Endl M, Strassmeier KG, Kürster M (1997) A large X-ray flare on HU Virginis. Astron Astrophys 328:565
Euchner F, Jordan S, Beuermann K, Gänsicke B, Hessman FV (2002) Zeeman tomography of magnetic white dwarfs. I. Reconstruction of the field geometry from synthetic spectra. Astron Astrophys 390:633
Evershed J (1910) Radial movement in sun-spots; second paper. MNRAS 70:217
Fluri DM, Berdyugina SV (2004) Flip-flops as observational signatures of different dynamo modes in cool stars. Sol Phys 224:153
Frasca A, Biazzo K, Taş G, Evren S, Lanzafama AC (2008) Spots, plages, and flares on λ Andromedae and II Pegasi. Astron Astrophys 479:557
Freytag B, Steffen M, Dorch B (2002) Spots on the surface of Betelgeuse—results from new 3D stellar convection models. Astronomische Nachrichten 323:213
Frick P, Soon WH, Popova E, Baliunas SL (2004) Time-spectra of chromospheric activity of old solar-type stars: detection of rotational signals from double wavelet analysis. N Astron 9:599
Fröhlich H-E, Kroll P, Strassmeier KG (2005) The RS CVn binary HK Lacertae: long-term photometry from Sonneberg sky-patrol plates. Astron Astrophys 454:295
Fröhlich H-E, Tschäpe R, Rüdiger G, Strassmeier KG (2002) EK Draconis: long-term photometry on Sonneberg Sky-Patrol plates. Astron Astrophys 391:659
Gilliland R, Dupree A (1996) First image of the surface of a star with the hubble space telescope. Astrophys J 463:L29
Gleissberg W (1958) The eighty-year sunspot cycle. J Br Astron Assoc 68:148
Gondoin P (1986) Active regions on HR 1099 from a high resolution spectroscopic study of photospheric (Fe I) and chromospheric (Ca II and H-alpha) lines. Astron Astrophys 160:73
Gray DF, Brown K (2001) Line-depth ratios: temperature indices for giant stars. PASP 113:723
Gray DF, Johanson HL (1991) Precise measurement of stellar temperatures using line-depth ratios. PASP 103:439
Güdel M (2007) The sun in time: activity and environment. Living Rev Sol Phys 4:3
Güdel M, Audard M, Smith KW et al (2003) A systematic spectroscopic X-ray study of stellar coronae with XMM-Newton: early results. In: Ayres T (ed) 12th Cambridge workshop, cool stars, stellar systems, and the sun. University of Colorado, p 303
Guinan EF, Güdel M, Kang YW, Margheim S (1997) Chromospherically active stars in the galactic bulge as source of the diffusive X-ray background. In: Ferlet R, Maillard JP, Raban B (eds) Variable stars and the astrophysical returns of microlensing surveys. Edition Frontiers, p 339
Hackman T, Jetsu L, Tuominen I (2001) Surface imaging of HD 199178 (V1794 Cygni). Astron Astrophys 374:171
Hall DS (1972) A T Tauri-like star in the eclipsing binary RS Canum Venaticorum. PASP 84:323
Hall DS, Busby MR (1990) Starspot lifetimes. In: Ibanoglu C (ed) Active close binaries, NATO ASI. Kluwer, Dordrecht, p 377
Hall DS, Henry GW (1994) The law of starspot lifetimes. IAPPP 55:51
Hartmann L, Dussault M, Noah PV, Klimke A, Bopp BW (1981) Evidence for a starspot cycle on BD +26 deg 730. Astrophys J 249:662
Hartman JD, Gaudi BS, Holman MJ et al (2008) Deep MMT transit survey of the open cluster M37. II. Variable stars. Astrophys J 675:1254
Hathaway DH, Choudhary DP (2008) Sunspot group decay. Sol Phys 250:269
Hatzes AP (1993) Doppler imaging stars with moderate rotation—the spot distribution on Sigma Geminorum. Astrophys J 410:777
Hatzes AP (1995) Doppler imaging of the cool spot distribution on the weak T Tauri star V410 Tauri. Astrophys J 451:784

Hatzes AP (1995a) Spot and chromospheric activity on the RS CVn star DM Ursae Majoris. Astron J 109:350
Hatzes AP (1995b) Doppler images of II Peg. In: Strassmeier KG (ed) Poster proceedings of IAU symposium 176. University of Vienna, Austria, p 87
Hatzes AP (1995c) Doppler images of the dMe binary YY Gem. In: Strassmeier KG (ed) Poster proceedings of IAU symposium 176. University of Vienna, Austria, p 90
Hatzes AP (1995d) Doppler imaging of the cool spot distribution on the weak T Tauri star V410 Tauri. Astrophys J 451:784
Hatzes AP (1998) Spot activity and the differential rotation on HD 106225 derived from Doppler tomography. Astron Astrophys 330:541
Hatzes AP (2001) Doppler imaging of the naked T Tauri star V830 Tau. In: Garcia Lopez R et al (eds) 11th Cambridge workshop, cool stars, stellar systems, and the sun, ASP conference series 223, CD-ROM, p 1244
Hatzes AP (2002) Starspots and exoplanets. Astronomische Nachrichten 323:392
Hatzes AP, Kürster M (1999) Doppler images of the pre-main sequence binary V824 Arae. Astron Astrophys 346:432
Hatzes AP, Vogt SS (1992) Doppler images of the spotted RS CVn star HD 26337—1984–1987. MNRAS 258:387
Hempelmann A, Hatzes AP, Kürster M, Patkos L (1995) Spots, plages, and coronal X-ray sources on SV Cam: results from a multi-wavelength campaign. In: Strassmeier KG (ed) Poster proceedings of IAU symposium 176. University of Vienna, Austria, p 194
Hempelmann A, Schmitt JHMM, Baliunas SL, Donahue RA (2003) Evidence for coronal activity cycles on 61 Cygni A and B. Astron Astrophys 406:L39
Hendry MA, Bryce HM, Valls-Gabaud D (2002) The microlensing signatures of photospheric starspots. MNRAS 335:539
Hendry PA, Mochnacki SW (2000) Doppler imaging of VW Cephei: distribution and evolution of starspots on a contact binary. Astrophys J 531:467
Henry GW, Baliunas SL, Donahue RA, Fekel FC, Soon W (2000) Photometric and Ca II H and K spectroscopic variations in nearby sun-like stars with planets. III. Astrophys J 531:415
Heyrovský D, Sasselov D (2000) Detecting stellar spots by gravitational microlensing. Astrophys J 529:69
Hoffmeister C (1965) Analyse der Lichtkurven von vier RW Aurigae-Sternen. Veröff Sternwarte Sonneberg 6:97
Holzwarth V, Mackay DH, Jardine M (2006) The impact of meridional circulation on stellar butterfly diagrams and polar caps. MNRAS 369:1703
Hubrig S, North P, Schöller M (2007) Evolution of magnetic fields in stars across the upper main sequence: II. Observed distribution of the magnetic field geometry. Astronomische Nachrichten 328:475
Huerta M, Johns-Krull C, Prato L, Hartigan P, Jaffe DT (2008) Starspot-induced radial velocity variability in LkCa 19. Astrophys J 678:472
Hussain GAJ (2002) Starspot lifetimes. Astronomische Nachrichten 323:349
Hussain GAJ, Allende Prieto C, Saar SH, Still M (2006) Spot patterns and differential rotation in the eclipsing pre-cataclysmic variable binary V471 Tau. MNRAS 367:1699
Hussain GAJ, Unruh YC, Collier Cameron A (1997) Doppler imaging of AB Doradus using the LiI 6708 line. MNRAS 288:343
Irwin J, Hodgkin S, Aigrain S et al (2007) The Monitor project: rotation of low-mass stars in the open cluster NGC2516. MNRAS 377:741
Işik E, Schüssler M, Solanki SK (2007a) Magnetic flux transport on active cool stars and starspot lifetimes. Astron Astrophys 464:1049
Işik E, Schmitt D, Schüssler M (2007b) A coupled model of magnetic flux generation and transport in stars. Astronomische Nachrichten 328:1111
Jankov S, Donati J-F (1995) Indirect surface imaging of HR 1099 from MUSICOS 1989 and 1992 data. Multi-site continuous spectroscopy. In: Proceedings of the 4th workshop held in Beijing, China, 19–24 June 1994, p 143
Järvinen SP, Berdyugina SV, Strassmeier KG (2005) Spots on EK Draconis. Active longitudes and cycles from long-term photometry. Astron Astrophys 440:735
Järvinen S, Korhonen H, Berdyugina SV, Ilyin I, Strassmeier KG, Weber M, Savanov I, Tuominen I (2008) Magnetic activity on V889 Herculis. Combining photometry and spectroscopy. Astron Astrophys 488:1047

Jeffers SV, Barnes JR, Collier Cameron A (2002) The latitude distribution of star-spots on He 699. MNRAS 331:666
Jeffers SV, Donati J-F, Collier Cameron A (2007) Magnetic activity on AB Doradus: temporal evolution of star-spots and differential rotation from 1988 to 1994. MNRAS 375:567
Jetsu L, Pelt J, Tuominen I, Nations H (1991) The spot activity of FK Comae Berenices. In: Tuominen I, Moss D, Rüdiger G (eds) The sun and cool stars. Activity, magnetism, dynamos. Proceedings of colloquium No. 130 of the international astronomical union. Springer, Berlin, New York, p 381
Johns-Krull C, Hatzes AP (1997) The classical T Tauri star Sz 68: Doppler imaging and evidence for magnetospheric accretion. Astrophys J 487:896
Johns Krull CM, Valenti JA, Saar SH (2004) Testing the reality of strong magnetic fields on T Tauri stars: the naked T Tauri star hubble 4. Astrophys J 617:1204
Joncour I, Bertout C, Bouvier J (1994a) Doppler imaging of the T Tauri star HDE 283572. Astron Astrophys 291:L19
Joncour I, Bertout C, Menard F (1994b) Doppler imaging of the T Tauri star V410 Tau. Astron Astrophys 285:L25
Jordan S (2009) Magnetic fields in white dwarfs and their direct progenitors. In: Strassmeier KG, Kosovichev A, Beckman J (eds) IAU symposium 259, cosmic magnetic fields: from planets, to stars and galaxies. Cambridge University Press, London, p 369
Kaiser ME, Kruk JW, McCandliss SR et al (2007) ACCESS—absolute color calibration experiment for standard stars. Bull AAS 211:1123
Kang YW, Wilson RE (1989) Least-squares adjustment of spot parameters for three RS CVn binaries. Astron J 97:848
Kashyap VL, Drake JJ, Saar SH (2008) Extrasolar giant planets and X-ray activity. Astrophys J 687:1339
Kitchatinov LL, Rüdiger G (2007) Sunspot models with bright rings. In: Kneer F, Puschmann K, Wittmann A (eds) Modern solar facilities—advanced solar science. Universitätsverlag Göttingen, p 343
Kochukhov O, Piskunov NE (2006) Magnetic Doppler imaging of active stars. In: IAU JD8, solar and stellar activity cycles, GA Prague, #7
Kolláth Z, Oláh K (2009) Multiple and changing cycles of active stars. I. Methods of analysis and application to the solar cycle. Astron Astrophys (submitted)
Korhonen H, Berdyugina SV, Hackman T, Duemmler R, Ilyin I, Tuominen I (1999) Study of FK Comae Berenices. I. Surface images for 1994 and 1995. Astron Astrophys 346:101
Korhonen H, Berdyugina SV, Hackman T, Strassmeier KG, Tuominen I (2000) Study of FK Comae Berenices. II. Spot evolution from 1994 to 1997. Astron Astrophys 360:1067
Korhonen H, Berdyugina SV, Strassmeier KG, Tuominen I (2001) The first close-up of the "flip-flop" phenomenon in a single star. Astron Astrophys 379:L30
Korhonen H, Elstner D (2005) Photometric observations from theoretical flip-flop models. Astron Astrophys 440:1161
Korhonen H, Hubrig S, Berdyugina SV et al (2009) First measurements of the magnetic field on FK Com and its relation to the contemporaneous starspot locations. MNRAS 395:282
Korhonen H, Järvinen S (2007) Active longitudes and flip-flops in binary stars. In: Hartkopf WI, Guinan EF, Harmanec P (eds) IAU symposium 240, binary stars as critical tools and tests in contemporary astrophysics. Cambridge University Press, London, p 453
Kosovichev AG (2002) Subsurface structure of sunspots. Astronomische Nachrichten 323:186
Kővári Zs, Strassmeier KG, Bartus J, Washuettl A, Weber M, Rice JB (2001) Doppler imaging of stellar surface structure. XVI. A time-series analysis of the moderately-rotating K1-giant sigma Geminorum. Astron Astrophys 373:199
Kővári Zs, Strassmeier KG, Granzer T, Weber M, Oláh K, Rice JB (2004) Doppler imaging of stellar surface structure. XXII. Time-series mapping of the young rapid rotator LQ Hydrae. Astron Astrophys 417:1047
Kővári Zs, Bartus J, Švanda M et al (2007a) Surface velocity network with anti-solar differential rotation on the active K-giant σ Geminorum. Astronomische Nachrichten 328:1081
Kővári Zs, Bartus J, Strassmeier KG, Oláh K, Weber M, Rice JB, Washuettl A (2007b) Doppler imaging of stellar surface structure. XXIII. The ellipsoidal K giant binary ζ Andromedae. Astron Astrophys 463:1071
Kővári Zs, Washuettl A, Foing BH et al (2008) Doppler maps and differential rotation of EI Eri from MUSICOS 1998 observations. Astron Astrophys (arXiv0811.0348, submitted)
Kron G (1947) The probable detecting of surface spots on AR Lacertae B. PASP 59:261

Küker M, Henning T, Rüdiger G (2003) Magnetic star-disk coupling in classical T Tauri systems. Astrophys J 589:397
Kürster M, Dennerl K (1993) Spatial correlations between coronal and photospheric active regions on late-type stars. In: Linsky JL, Serio S (eds) Physics of solar and stellar coronae: G. S. Vaiana memorial symposium, astrophysics and space science library, vol 183. Kluwer, Dordrecht, p 443
Kürster M, Hatzes AP, Pallavicini R, Randich S (1992) A comparison of star spot distributions for various active stars based on Doppler images. In: 7th Workshop on cool stars, stellar systems, and the sun, ASPC 26, p 249
Kürster M, Schmitt JHMM, Cutispoto G (1994) Doppler imaging with a CLEAN-like approach. II: a photospheric image of AB Doradus (=HD 36705). Astron Astrophys 289:899
Landstreet JD, Silaj J, Abdretta V et al (2008) Searching for links between magnetic fields and stellar evolution. III. Measurement of magnetic fields in open cluster Ap stars with ESPaDOnS. Astron Astrophys 481:465
Lanza AF (2008) Hot Jupiters and stellar magnetic activity. Astron Astrophys 487:1163
Lanza AF, Pagano I, Leto G, Messina S, Barge P, Baglin A et al (2009) Magnetic activity in the photosphere of CoRoT-Exo-2a. Active longitudes and short-term spot cycle in a young sun-like star. Astron Astrophys 493:193
Le Bouquin J-B, Bauvir B, Haguenauer P, Schöller M, Rantakyrö F, Menardi S (2008) First result with AMBER+FINITO on the VLTI: the high-precision angular diameter of V3879 Sagittarii. Astron Astrophys 481:553
Lister TA, Collier Cameron A, Bartus J (1999) Doppler imaging of BD+22deg4409 (LO Peg) using least-squares deconvolution. MNRAS 307:685
Li LH, Ventura P, Basu S, Sofia S, Demarque P (2006) Two-dimensional stellar evolution code including arbitrary magnetic fields. I. Mathematical techniques and test cases. Astrophys J Suppl 164:215
Lobel A, Aufdenberg J, Dupree AK, Kurucz RL, Stefanik RP, Torres G (2004) Spatially resolved STIS spectroscopy of Betelgeuse's outer atmosphere. In: Dupree AK, Benz AO (eds) IAU symposium 219, stars as suns: activity, evolution and planets, ASPC, p 641
Lockwood GW, Radick RR, Henry GW, Baliunas SL (2004) A comparison of solar irradiance variations with those of similar stars. Bull AAS 204:304
Lockwood GW, Skiff BA, Henry GW, Henry S, Radick R R, Baliunas SL, Donahue RA, Soon W (2007) Patterns of photometric and chromospheric variation among sun-like stars: a 20 year perspective. Astrophys J Suppl 171:260
Loughhead RE, Bray RJ (1958) The Wilson effect in sunspots. Aust J Phys 11:177
Maceroni C, Vilhu O, van't Veer F, van Hamme W (1994) Surface imaging of late-type contact binaries I: AE Phoenicis and YY Eridani. Astron Astrophys 288:529
Maeder A, Meynet G (2004) Stellar evolution with rotation and magnetic fields. II. General equations for the transport by Tayler-Spruit dynamo. Astron Astrophys 422:225
Maeder A, Meynet G, Georgy C, Ekström S (2009) The basic role of magnetic fields in stellar evolution. In: Strassmeier KG, Kosovichev A, Beckman J (eds) IAU symposium 259, cosmic magnetic fields: from planets, to stars and galaxies. Cambridge University Press, London, p 311
Marsden SC, Waite IA, Carter BD, Donati J-F. (2004) Doppler imaging of G-dwarfs in two young open clusters. Astronomische Nachrichten 325:246
Marsden SC, Waite IA, Carter BD, Donati J-F (2005) Doppler imaging and surface differential rotation of young open cluster stars—I. HD 307938 (R58) in IC 2602. MNRAS 359:711
Marsden SC, Donati J-F, Semel M, Petit P, Carter BD (2006) Surface differential rotation and photospheric magnetic field of the young solar-type star HD 171488 (V889 Her). MNRAS 370:468
Marsden SC, Berdyugina SV, Donati J-F, Eaton JA, Williamson MH (2007) Starspots and relativity: applied Doppler imaging for the Gravity Probe B mission. Astronomische Nachrichten 328:1047
Martinez González MJ, Asensio Ramos A, Carroll TA, Kopf M, Ramirez Vélez JC, Semel M (2008) PCA detection and denoising of Zeeman signatures in stellar polarized spectra. Astron Astrophys 486:637
Martínez Pillet V, Moreno Insertis F, Vázquez M (1993) The distribution of sunspot decay rates. Astron Astrophys 274:521
Meibom S, Mathieu RD, Stassun KG (2008) Stellar rotation in M35: mass-period relations, spin-down rates, and gyrochronology. astro-ph/0805.1040
Messina S, Guinan EF (2002) Magnetic activity of six young solar analogues I. Starspot cycles from long-term photometry. Astron Astrophys 393:225

Messina S, Guinan EF, Lanza AF, Ambruster C (1999) Activity cycle and surface differential rotation of the single Pleiades star HD 82443 (DX Leo). Astron Astrophys 347:249
Montmerle T (2003) The role of accretion disks in the coronal activity of young stars. Adv Space Res 32(6):1067
Morales JC, Ribas I, Jordi C (2008) The effect of activity on stellar temperatures and radii. Astron Astrophys 478:507
Morales JC, Ribas I, Jordi C et al (2009) Absolute properties of the low-mass eclipsing binary CM Draconis. Astrophys J 691:1400
Morin J, Donati J-F, Forveille T et al (2008) The stable magnetic field of the fully convective star V374 Peg. MNRAS 384:77
Moss D (2004) Dynamo models and the flip-flop phenomenon in late-type stars. MNRAS 352:L17
Mullan DJ (1975) On the possibility of magnetic starspots on the primary components of W Ursae Majoris type binaries. Astrophys J 198:563
Neuhäuser R, Wolk SJ, Torres G et al (1998) Optical and X-ray monitoring, Doppler imaging, and space motion of the young star Par 1724 in Orion. Astron Astrophys 334:873
Noah PV, Bopp BW, Fekel FC (1987) Doppler snapshots. In: 5th Cambridge workshop on cool stars, stellar systems and the sun, Colorado University
Oláh K, Jurcsik J, Strassmeier KG (2003) Differential rotation on UZ Librae. Astron Astrophys 410:685
Oláh K, Kolláth Z, Strassmeier KG (2000) Multiperiodic light variations of active stars. Astron Astrophys 356:643
Oláh K, Kolláth Z, Granzer T et al (2009) Multiple and changing cycles of active stars. II. Results. Astron Astrophys (submitted)
Oláh K, Strassmeier KG (1992) On the starspot temperature of HD 12545. Astron Astrophys 259:595
Oláh K, Strassmeier KG (2002) Starspot cycles from long-term photometry. Astronomische Nachrichten 323:361
Oláh K, Strassmeier KG, Granzer T, Soon W, Baliunas SL (2007) Changing stellar activity cycles. Astronomische Nachrichten 328:1072
Oláh K, Strassmeier KG, Kővári Zs, Guinan EF (2001) Time-series photometric spot modeling. IV. The multi-periodic K5Ve binary V833 Tauri. Astron Astrophys 372:119
Oláh K, Strassmeier KG, Weber M (2002) Doppler imaging of stellar surface structure. XVIII. The very active RS CVn binary UZ Librae revisited. Astron Astrophys 389:202
O'Neal D, Saar SH, Neff JE (1996) Measurements of starspot area and temperature on five active, evolved stars. Astrophys J 463:766
O'Neal D, Neff JE, Saar SH, Cuntz M (2004) Further results of TiO-band observations of starspots. Astron J 128:1802
Parker EN (1955) Hydromagnetic dynamo models. Astrophys J 122:293
Parker EN (1979) Sunspots and the physics of magnetic flux tubes. I—The general nature of the sunspot. II—Aerodynamic drag. Astrophys J 230:905
Peristykh AN, Damon PE (2003) Persistence of the Gleissberg 88-year solar cycle over the last ∼12,000 years: Evidence from cosmogenic isotopes. JGRA 108:1003
Petit P, Donati J-F, Wade GA et al (2004a) Magnetic topology and surface differential rotation on the K1 subgiant of the RS CVn system HR 1099. MNRAS 348:1175
Petit P, Donati J-F, Oliveira JM et al (2004b) Photospheric magnetic field and surface differential rotation of the FK Com star HD 199178. MNRAS 351:826
Petrov PP, Gullbring E, Gahm G et al (1995) Wind, accretion and spots of the T Tauri star SU Aurigae. In: Strassmeier KG (ed) Poster proceedings of IAU symposium 176, University of Vienna, p 217
Phillips MJ, Hartmann L (1978) Long-term variability of dMe stars. Astrophys J 224:182
Piluso N, Lanza AF, Pagano I, Lanzafama AC, Donati J-F (2008) Doppler imaging of the young late-type star LO Pegasi (BD+22°4409) in 2003 September. MNRAS 387:237
Piskunov NE (1991) The art of surface imaging. In: Tuominen I, Moss D, Rüdiger G (eds) IAU colloquium No. 130, the sun and cool stars. Activity, magnetism, dynamos. Springer, Berlin, p 309
Piskunov NE (1996) Doppler imaging of eclipsing binaries. In: Strassmeier KG, Linsky JL (eds) IAU symposium 176, stellar surface structure. Kluwer, Dordrecht, p 45
Piskunov NE, Huenemoerder DP, Saar SH (1994) Simultaneous spot and chromosphere maps of FK Comae. In: Caillault J-P (ed) 8th Cambridge workshop, cool stars, stellar systems, and the sun, astronomical society of the pacific conference Series, vol 64, p 658
Piskunov NE, Tuominen I, Vilhu O (1990) Surface imaging of late-type stars. Astron Astrophys 230:363

Piskunov NE, Vincent A, Duemmler R et al (2001) Doppler imaging of eclipsing binary systems ER Vul and TY Pyx. In: Garcia Lopez R et al (eds) 11th Cambridge workshop, cool stars, stellar systems, and the sun, ASP Conference Series 223, CD-ROM, p 1285
Piskunov NE, Kochukhov O (2002) Doppler imaging of stellar magnetic fields. I. Techniques. Astron Astrophys 381:736
Piskunov NE, Rice JB (1993) Techniques for surface imaging of stars. PASP 105:1415
Petrovay K, Van Driel-Gesztelyi L (1997) Making sense of sunspot decay. I. Parabolic decay law and Gnevyshev-Waldmeier relation. Sol Phys 176:249
Petrovay K, Martinez-Pillet V, Van Driel-Gesztelyi L (1999) Making sense of sunspot decay—II. Deviations from the mean law and Plage effects. Sol Phys 188:315
Poe CH, Eaton JA (1985) Starspot areas and temperatures in nine binary systems with late-type components. Astrophys J 289:644
Pojmanski G (2005) All sky automated survey catalog, VizieR online
Pont F, Gilliland RL, Moutou C et al (2007) Hubble space telescope time-series photometry of the planetary transit of HD 189733: no moon, no rings, starspots. Astron Astrophys 476:1347
Queloz D, Henry GW, Sivan JP et al (2001) No planet for HD 166435. Astron Astrophys 379:279
Radick RR, Thompson DT, Lockwood GW, Duncan DK, Baggett WE (1987) The activity, variability, and rotation of lower main-sequence Hyades stars. Astrophys J 321:459
Rámirez Velez JC, Semel M, Stift MJ, Leone F (2006) PCA technique applied to the detection of ZDI circular polarization in solar-type stars. In: Casini R, Lites BW (eds) Solar polarization 4, Boulder, ASPC 358, p 405
Ramsey LW, Nations HL (1980) HR 1099 and the starspot hypothesis for RS Canum Venaticorum binaries. Astrophys J 239:L121
Ramseyer TF, Hatzes AP, Jablonski F (1995) Doppler imaging of V471 Tau. Astron J 110:1364
Rempel M, Schüssler M, Knölker M (2009) Radiative MHD simulation of sunspot structure. Astrophys J 691:640
Rogers ML, Richards MT, Richards DSP (2006) Long-term Variability in the length of the solar cycle. astro-ph/0606426
Rice JB (2002) Doppler imaging of stellar surfaces—techniques and issues. Astronomische Nachrichten 323:220
Rice JB, Strassmeier KG (1996) Doppler imaging of stellar surface structure. II. The weak-lined T Tauri star V410 Tauri. Astron Astrophys 316:164
Rice JB, Strassmeier KG (1998) Doppler imaging of stellar surface structure. VII. The very young, single K2-dwarf LQ Hydrae. Astron Astrophys 336:972
Rice JB, Strassmeier KG (2001) Doppler imaging of stellar surface structure. XVII. The solar-type Pleiades star HII 314 = V1038 Tauri. Astron Astrophys 377:264
Rüdiger G, Hollerbach R (2004) The magnetic universe. Wiley-VCH, Berlin
Rüdiger G, Kitchatinov LL (2000) Sunspot decay as a test of the eta-quenching concept. Astronomische Nachrichten 321:75
Saar SH, Brandenburg A (1999) Time evolution of the magnetic activity cycle period. II. Results for an expanded stellar sample. Astrophys J 524:295
Saar SH, Brandenburg A (2002) A new look at dynamo cycle amplitudes. Astronomische Nachrichten 323:357
Saar SH, Donahue RA (1997) Activity-related radial velocity variation in cool stars. Astrophys J 485:319
Saar SH, Piskunov NE, Tuominen I (1994) Multi-epoch magnetic surface images of LQ Hya. In: Caillault J-P (ed) 8th Cambridge workshop, cool stars, stellar systems, and the sun, astronomical society of the pacific conference series, vol 64, p 661
Savanov IS, Strassmeier KG (2005) Surface imaging with atomic and molecular features. I. A new inversion technique and first numerical tests. Astron Astrophys 444:931
Savanov IS, Strassmeier KG (2008) Light-curve inversions with truncated least-squares principal components: tests and application to HD 291095 = V1355 Orionis. Astronomische Nachrichten 329:364
Scholz A, Eislöffel J (2007) The first rotation periods in Praesepe. MNRAS 381:1638
Schrijver CJ, Title AM (2001) On the formation of polar spots in sun-like stars. Astrophys J 551:1099
Schrijver CJ, Zwaan C (2000) Solar and stellar magnetic activity. Cambridge University Press, New York
Semel M (1989) Zeeman-Doppler imaging of active stars. I—basic principles. Astron Astrophys 225:456
Shkolnik E, Walker GAH, Bohlender DA (2003) Evidence for planet-induced chromospheric activity on HD 179949. Astrophys J 597:1092

Shulyak D, Khan S, Kochukhov O (2009) Advanced model atmospheres with magnetic field effects included. In: Strassmeier KG, Kosovichev A, Beckman J (eds) IAU symposium 259, cosmic magnetic fields: from planets, to stars and galaxies. Cambridge University Press, London, p 407
Silva-Valio A (2008) Estimating stellar rotation from starspot detection during planetary transits. Astrophys J 683:179
Skelly MB, Unruh YC, Collier Cameron A, Barnes J, Donati J-F, Lawson WA, Carter BD (2008) Doppler images and chromospheric variability of TWA 6. MNRAS 385:708
Solanki SK (2003) Sunspots: an overview. Astron Astrophys Rev 11:153
Solanki SK (2004) The magnetic field from the solar interior to the heliosphere. In: Poletto G, Suess ST (eds) The sun and the heliosphere as an integrated system. Astrophys Space Sci 317:373
Solanki SK, Unruh YC (2004) Spot sizes on sun-like stars. MNRAS 348:307
Stenflo JO (2002) Polarized radiation diagnostics of solar magnetic fields. In: Trujillo-Bueno J et al (eds) Astrophysical spectro-polarimetry. XII Canary Islands Winter School, Cambridge University Press, London, p 55
Stenflo JO (2004) Solar physics: hidden magnetism. Nature 430:304
Stempels HC, Gahm GF (2004) The close T Tauri binary V 4046 Sagittarii. Astron Astrophys 421:1159
Stępień K (1993) HR 1362: the evolved 53 Camelopardalis. Astrophys J 416:368
Stix M (2002) Sunspots: what is interesting? Astronomische Nachrichten 323:178
Stout-Batalha N (1997) Doppler imaging of young late-type stars: HII 686, HII 3163, and P1724. PhD Thesis, University of California
Stout-Batalha NM, Vogt SS (1999) Doppler imaging of two zero-age main-sequence stars in the Pleiades: HII 686 and HII 3163. Astrophys J Suppl 123:251
Strassmeier KG (1990) Photometric and spectroscopic modeling of starspots on the RS Canum Venaticorum binary HD 26337. Astrophys J 348:682
Strassmeier KG (1992) Starspot photometry - Observational review and interplay with spectroscopy. In: Filippenko A (ed) Proceedings of the 103rd ASP meeting, robotic telescopes for the 1990's, ASPC 34, p 39
Strassmeier KG (1994) Rotational-modulation mapping of the active atmosphere of the RS Canum Venaticorum binary HD 106225. Astron Astrophys 281:395
Strassmeier KG (1996) Doppler imaging of stellar surface structure. I. The rapidly-rotating RS CVn binary UZ Librae. Astron Astrophys 314:558
Strassmeier KG (1997) Doppler imaging of stellar surface structure. III. The X-ray source HD 116544 = IN Virginis. Astron Astrophys 319:535
Strassmeier KG (1999) Doppler imaging of stellar surface structure. XI. The super starspots on the K0 giant HD 12545: larger than the entire Sun. Astron Astrophys 347:225
Strassmeier KG (2000) Doppler imaging of stellar surface structure. XIII. The flaring RS CVn-binary HD 291095 = V1355 Orionis. Astron Astrophys 357:608
Strassmeier KG (2002) Doppler images of starspots. Astronomische Nachrichten 323:309
Strassmeier KG (2005) Stellar activity cycles: observing the dynamo? Astronomische Nachrichten 326:269
Strassmeier KG, Bartus J (2000) Doppler imaging of stellar surface structure. XII. Rapid spot changes on the RS CVn binary V711 Tauri = HR 1099. Astron Astrophys 354:537
Strassmeier KG, Bartus J, Kővari Zs, Weber M, Washuettl A (1998) Doppler imaging of stellar surface structure. VIII. The effectively single and rapidly-rotating G8-giant HD 51066 = CM Camelopardalis. Astron Astrophys 336:587
Strassmeier KG, Bopp BW (1992) Time-series photometric spot modeling. I—parameter study and application to HD 17433 = VY Arietis. Astron Astrophys 259:183
Strassmeier KG, Granzer T, Weber M et al (2004) The STELLA robotic observatory. Astronomische Nachrichten 325:527
Strassmeier KG, Hall DS, Fekel FC, Scheck M (1993a) A catalog of chromospherically active binary stars (second edition). Astron AstrophysS 100:173
Strassmeier KG, Hall DS, Henry GW (1994a) Time-series photometric spot modeling. II: fifteen years of photometry of the bright RS CVn binary HR 7275. Astron Astrophys 282:535
Strassmeier KG, Hubl B, Rice JB (1997) Doppler imaging of stellar surface structure. IV. The rapidly-rotating G5III-IV star HD 112313 = IN Comae. Astron Astrophys 322:511
Strassmeier KG, Kratzwald L, Weber M (2003a) Doppler imaging of stellar surface structure. XX. The rapidly-rotating single K2-giant HD 31993 = V1192 Orionis. Astron Astrophys 408:1103
Strassmeier KG, Lupinek S, Dempsey RC, Rice JB (1999a) Doppler imaging of stellar surface structure. X. The FK Comae-type star HD 199178 = V 1794 Cygni. Astron Astrophys 347:212

Strassmeier KG, Pichler T, Weber M, Granzer T (2003b) Doppler imaging of stellar surface structure. XXI. The rapidly-rotating solar-type star HD 171488 = V889 Hercules. Astron Astrophys 411:595
Strassmeier KG, Rice JB (1998a) Doppler imaging of stellar surface structure. VI. HD 129333 = EK Draconis: a stellar analog of the active young Sun. Astron Astrophys 330:685
Strassmeier KG, Rice JB (1998b) Doppler imaging of stellar surface structure. IX. A high-resolution image of the weak-lined T Tauri star HDE 283572 = V987 Tauri. Astron Astrophys 339:497
Strassmeier KG, Rice JB (2000) Doppler imaging of stellar surface structure. XIV. The double-lined pre-main-sequence binary V 824 Arae = HD 155555. Astron Astrophys 360:1019
Strassmeier KG, Rice JB (2003) Doppler imaging of stellar surface structure. XIX. The solar-type components of the close binary σ^2 Coronae Borealis. Astron Astrophys 399:315
Strassmeier KG, Rice JB (2006) First Doppler images of the very young K2-dwarf PW Andromedae = HD 1405. Astron Astrophys 460:751
Strassmeier KG, Rice JB, Ritter A, Küker M, Hussain GAJ, Hubrig S, Shobbrook R (2005) Spatially resolving the accretion shocks on the rapidly-rotating M0 T-Tauri star MN Lupi. Astron Astrophys 440:1105
Strassmeier KG, Rice JB, Wehlau W et al (1991) Doppler imaging of high-latitude spot activity on HD 26337. Astron Astrophys 247:130
Strassmeier KG, Rice JB, Wehlau W et al (1993b) Surface features of the lower atmosphere of HD 82558 (= LQ Hydrae). Astron Astrophys 268:671
Strassmeier KG, Schordan P (2000) A temperature calibration for MK-class III giants from high-resolution spectral line-depth ratios. Astronomische Nachrichten 321:277
Strassmeier KG, Stępień K, Henry GW, Hall DS (1999b) Evolved, single, slowly rotating …but magnetically active. The G8-giant HR 1362 = EK Eridani revisited. Astron Astrophys 343:175
Strassmeier KG, Welty AD, Rice JB (1994b) A Doppler image of the weak T Tauri star V410 Tau. Astron Astrophys 285:L17
Švanda M, Klvaňa M, Sobotka M (2006) Large-scale horizontal flows in the solar photosphere. I. Method and tests on synthetic data. Astron Astrophys 458:301
Thomas JH, Weiss NO (2008) Sunspots and starspots, Cambridge astrophysics series 46. Cambridge University Press, London
Toner CG, Gray DF (1988) The starpatch on the G8 dwarf XI Bootis A. Astrophys J 334:1008
Toner CG, LaBonte BJ (1990) Xi-Bootis—starpatch or moat flow. In: Wallerstein G (ed) 6th Cambridge workshop, cool stars, stellar systems, and the sun. Kluwer, Dordrecht, ASPC 9, p 161
Tritschler A, Schmidt W (2002) Sunspot photometry with phase diversity. I. Methods and global sunspot parameters. Astron Astrophys 382:1093
Trujillo Bueno J (2009) UV-Optical-IR spectropolarimetry. In: Strassmeier KG, Kosovichev A, Beckman J (eds) IAU symposium 259, cosmic magnetic fields: from planets, to stars and galaxies. Cambridge University Press, London, p 623
Tsuneta S, Ichimoto K, Katsukawa Y et al (2008) The magnetic landscape of the Sun's polar region. Astrophys J 688:1374
Unruh YC, Collier Cameron A, Cutispoto G (1995) The evolution of surface structures on AB-Doradus. MNRAS 277:1145
Unruh YC, Collier Cameron A (1997) Does chromospheric emission mimic polar starspots in Doppler images? MNRAS 290:37
Unruh YC, Collier-Cameron A, Guenther E (1998) Surface inhomogeneities and line variability on DF Tau. MNRAS 295:781
Unruh YC, Donati J-F, Oliviera J et al (2004) Multisite observations of SU Aurigae. MNRAS 348:1301
Unruh YC, Gatti AA, Drew JE et al (2001) Doppler images of LW Hydrae. In: Garcia Lopez R et al (eds) 11th Cambridge workshop, cool stars, stellar systems, and the sun, ASP conference series 223, CD-ROM, p 1320
Vida K, Kővári Zs, Švanda M et al (2007) Anti-solar differential rotation and surface flow pattern on UZ Libræ. Astronomische Nachrichten 328:1078
Vogt SS (1979) A spectroscopic and photometric study of the star spot on HD 224085. PASP 91:616
Vogt SS (1981a) Starspots—a review of observations and theory. In: The physics of sunspots. Sacramento Peak Observatory, p 455
Vogt SS (1981b) A spectroscopic, photometric, and magnetic study of the starspot on II Pegasi. Astrophys J 247:975

Vogt SS (1988) Doppler images of spotted late-type stars. In: Cayrel de Strobel G, Spite M (eds) IAU symposium 132, the impact of very high S/N spectroscopy on stellar physics. Kluwer, Dordrecht, p 253
Vogt SS, Hatzes AP (1991) The differential rotation and evolution of spots on UX-Arietis from a sequence of Doppler images. In: Tuominen I, Moss D, Rüdiger G (eds) IAU colloquium 130, the sun and cool stars: activity, magnetism, dynamos. Springer, New York, p 297
Vogt SS, Hatzes A, Misch A, Kürster M (1999) Doppler imagery of the spotted RS Canum Venaticorum star HR 1099 (V711 Tauri) from 1981 to 1992. Astrophys J Suppl 121:547
Vogt SS, Penrod GD (1983) Doppler imaging of spotted stars—application to the RS Canum Venaticorum star HR 1099. PASP 95:565
Walker GH, Croll B, Kuschnig R et al (2007) The differential rotation of κ^1-Ceti as observed by MOST. Astrophys J 659:1611
Washuettl A, Strassmeier KG (2001) A study of the chromospherically active binaries UX Fornacis and AG Doradus. Astron Astrophys 370:218
Washuettl A, Strassmeier KG, Foing BH et al (2003) MUSICOS observations of the chromospherically active binary star EI Eridani. In: Brown A et al (eds), 12th Cambridge workshop, cool stars, stellar systems, and the sun. University of Colorado, p 1008
Washuettl A, Strassmeier KG, Weber M, Kővári Zs (2009) The chromospherically active binary star EI Eridani. II. Long-term Doppler imaging. Astronomische Nachrichten 330:366
Watson CA, Dhillon VS, Shahbaz T (2006) Roche tomography of cataclysmic variables—III. Starspots on AE Aqr. MNRAS 368:637
Watson CA, Steeghs D, Shahbaz T, Dhillon VS (2007a) Roche tomography of cataclysmic variables—IV. Starspots and slingshot prominences on BV Cen. MNRAS 382:1105
Watson CA, Steeghs D, Dhillon VS, Shahbaz T (2007b) Imaging the cool stars in the interacting binaries AE Aqr, BV Cen and V426 Oph. Astronomische Nachrichten 328:813
Weber M (2004) Robotic telescopes and Doppler imaging: measuring differential rotation on long-period active stars. PhD thesis, University of Potsdam
Weber M (2007) Differential rotation of giant stars. Astronomische Nachrichten 328:1075
Weber M, Strassmeier KG (1998) Doppler imaging of stellar surface structure. V. The long-period RS CVn binary HD81410 = IL Hydrae. Astron Astrophys 330:1029
Weber M, Strassmeier KG (2001) Doppler imaging of stellar surface structure. XV. A possible detection of differential rotation and meridional flows on the rapidly rotating giant HD218153 = KU Pegasi. Astron Astrophys 373:974
Weber M, Strassmeier KG, Granzer T (2009) Time-series Doppler imaging with STELLA. In: Strassmeier KG, Kosovichev A, Beckman J (eds) IAU symposium 259, cosmic magnetic fields: from planets, to stars and galaxies. Cambridge University Press, London, p 427
Weber M, Washuettl A, Strassmeier KG (2001) Doppler images of HD218153 and HK Lac. In: Garcia Lopez R et al (eds) 11th Cambridge workshop, cool stars, stellar systems, and the sun, ASP conference series 223, CD-ROM
Wickramasinghe DT, Ferrario L (2000) Magnetism in isolated and binary white dwarfs. PASP 112:873
Wielebinski R, Beck R (eds) (2005) Cosmic magnetic fields, lecture notes in physics, vol 664. Springer, Berlin
Wilson OC (1968) Flux measurements at the centers of stellar H- and K-lines. Astrophys J 153:221
Wittkowski M, Langer N, Weigelt G (1998) Diffraction-limited speckle-masking interferometry of the red supergiant VY CMa. Astron Astrophys 340:L39
Wittkowski M, Schöller M, Hubrig S, Posselt B, von der Lühe O (2002) Measuring starspots on magnetically active stars with the VLTI. Astronomische Nachrichten 323:241
Wittkowski M, Boboltz DA, Driebe T, Le Bouquin J-B, Millour F, Ohnaka K, Scholz M (2008) J, H, K spectro-interferometry of the Mira variable S Orionis. Astron Astrophys 479:L21
Wolter U, Robrade J, Schmitt JHMM, Ness JU (2008) Doppler imaging an X-ray flare on the ultrafast rotator BO Mic. A contemporaneous multiwavelength study using XMM-Newton and VLT. Astron Astrophys 478:L11
Wolter U, Schmitt JHMM, vanWyk F (2005) Doppler imaging of Speedy Mic using the VLT. Fast spot evolution on a young K-dwarf star. Astron Astrophys 435:261
Wozniak PR, Udalski A, Szymanski M, Kubiak M, Pietrzynski G, Soszinski I, Zebrun K (2005) DIA OGLE-2 catalog, VizieR online

Wright JT, Marcy GW, Butler R, Vogt SS (2004) Chromospheric Ca II emission in nearby F, G, K, and M stars. Astrophys J Suppl 152:264

Zboril M, Byrne PB, Amado PJ (1998) Mapping stellar surface structures on the RS CVn Star II Peg. In: Donahue RA, Bookbinder JA (eds) The tenth cambridge workshop on cool stars, stellar systems and the sun. ASP Conf Ser, vol 154, p 2082

Zhao J, Kosovichev AG, Duvall TL Jr (2001) Investigation of mass flows beneath a sunspot by time-distance helioseismology. Astrophys J 557:384

Ziegler U (2005) Self-gravitational adaptive mesh magnetohydrodynamics with the NIRVANA code. Astron Astrophys 435:385